M-Pos516

INFLUENCE OF HALOTHANE ON SPEED OF SHORTENING OF RAT CARDIAC MUSCLE. F. Julian, S. Striz, J. Herland & R. Maddi. Dept. of Anesthesiology, Brigham & Women's Hospital, Boston, MA 02115.

Much evidence indicates that the vapor anesthetics, Halothane (HAL), Enflurane & Isoflurane, depress force generation (FG) in cardiac muscle, but it is unclear whether the decreased speed of shortening (SOS) also reported results from an additional specific effect of these vapors on cross-bridge cycling rate. We studied rat papillary muscles contracting at 12/min in Krebs-Ringer solution (KRS) at 30°C. Techniques for mounting, stimulation and measuring force and speed have been described (Julian et al., Circ. Res., 1981, 49, 1300). HAL was added to KRS to make its concentration 0.57 mM - a value near the minimal observed during anesthesia. This caused marked depression of FG (77%) & SOS (58%). A similar reduction in FG (76%) was caused by omitting HAL and lowering the $[Ca^{2+}]$ in KRS from 2.5 to 1.13 mM (LCA). HAL & LCA depressed d(FG)/dt similarly. The SOS decrease caused by LCA was exactly the same as that caused by HAL in normal KRS - 58%. Values are means for n=6 & SEM's ≤ 7% of means. These results indicate that it is not necessary to assume an additional influence of HAL on SOS, since LCA treatment which depressed FG & d(FG)/dt to the same degree as HAL alone caused exactly the same decrease of SOS. However, detailed analysis of the depressed FG's reveals subtle differences indicating the effects of HAL & LCA are not identical. Supported by NIH HL-35032.

M-Pos517

BAY K 8644 MAY AFFECT CARDIAC SR VIA DIRECT COMMUNICATION BETWEEN SARCOLEMMAL AND SR Ca CHANNELS. Larry V. Hryshko, Virginia M. Stiffel and Donald M. Bers. Div. Biomed. Sci. Univ. of CA, Riverside CA 92521.

In ferret myocardium, short rest periods lead to contractile potentiation. This rest potentiation is converted to rest depression by 1μM BAY k 8644 (BAY). This effect is similar to that observed for agents known to impair SR function (e.g. ryanodine, RY). During depressed postrest contractions, action potential amplitude and duration are increased. Since BAY increases I_{Ca}, we tested whether rest depression was due to a supra-optimal I_{Ca} "trigger" for SR Ca release. Whole cell I_{Ca} measurements revealed that both control and BAY treated myocytes exhibit decreased post-rest I_{Ca}, excluding this possibility. Rapid cooling contractures indicated that BAY accelerates the loss of SR Ca during rest. As BAY does not appear to affect isolated SR, we hypothesized that intact coupling between the SR and the sarcolemma is required. To test this, ^{3}H-RY binding was examined in isolated ferret myocytes and rabbit skeletal muscle triads. In both preparations, RY binding was increased in the presence of BAY. ATP also increased RY binding to triads, but inhibited the ability of BAY to stimulate RY binding. Under conditions expected to decrease triad integrity, the ability of either BAY or ATP to increase RY binding was lost. These results raise the possibility that occupancy of the DHP receptor by BAY may modulate the properties of the SR Ca release channel.

M-Pos518

RELATIONSHIP BETWEEN i_{Ca} AND Ca^{2+}-RELEASE IN VOLTAGE CLAMPED RAT VENTRICULAR CELLS. L. Cleemann and M. Morad. Department of Physiology, University of Pennsylvania, Philadelphia, PA 19104.

The time and voltage dependence of i_{Ca} was compared to SR Ca^{2+} release estimated from cell shortening and Ca^{2+} transients measured with fura-2 (K_d=0.14 uM) or mag-fura-2 (K_d=44 uM). Both Ca^{2+} probes showed that the Ca^{2+} transient at 0 mV had a delay (D) of 8 ms and a time constant (T) of 12 ms. The known activation and inactivation kinetics of i_{Ca} were mirrored by Ca^{2+} transients which: 1) had shorter D but longer T at positive potentials, 2) had shorter D when Ca^{2+} channel had been opened by a conditioning pulse near E_{Ca} (60 mV), and 3) arrested its development when Ca^{2+} was terminated by repolarization to potentials <-40 mV or depolarization to +100 mV. The voltage dependence of the fura-2 transient measured 25 ms after depolarization correlated with the integral of i_{Ca} measured prior to this time while the peak cell shortening measured 100 ms later correlated with simultaneous estimates of $[Ca^{2+}]_i$. These findings are consistent with the hypothesis that the release of Ca^{2+} from the SR is directly regulated by Ca^{2+} influx through the Ca^{2+} channel.

M-Pos519

INOSITOL (1,4,5)TRISPHOSPHATE DOES NOT ENHANCE Ca^{2+} SENSITIVITY OF Ca^{2+}-INDUCED Ca^{2+} RELEASE FROM MYOCARDIAL SARCOPLASMIC RETICULUM. Y. Zhu and T.M. Nosek, Dept. of Physiol./ Endo., Med. College of GA., Augusta, GA, 30912

An earlier report from this lab (Am. J. Physiol. 250:C807, 1986) found that IP3 enhanced spontaneous Ca^{2+} release and caffeine sensitivity of Ca^{2+} release from myocardial SR. We tested whether these effects were due to an increase in the Ca^{2+} sensitivity of the Ca^{2+}-induced-Ca^{2+} release (CICR) process by quantifying the SR Ca^{2+} content of saponin-skinned rat papillary muscles (from the mechanical response to 50 mM caffeine in a low EGTA medium) under various conditions. We found that: i) half maximal CICR is at pCa 5.64; ii) maximal CICR is at pCa 5 while higher Ca^{2+} inhibits CICR; iii) 10 mM Mg^{2+} decreases CICR; iv) 5 mM caffeine increases CIRC; v) 30 μM **IP3 has no significant effect on calcium sensitivity of CICR.** Two possible explanations for the lack of an IP3 effect (GTP dependence of release or rapid IP3 hydrolysis) were ruled out; the response to IP3 was unaffected by GTP, GTPγS, Ni^{2+}, Cd^{2+}, or 2,3,-diphosphoglycerate. Therefore, while IP3 influences Ca^{2+} release from the SR of skinned cardiac fibers, it does not do so by increasing the Ca^{2+} sensitivity of the CICR process. (Support: NIH HL/AR 37022, Am. Heart Assoc.-GA. Affil.)

M-Pos520

IMAGE ANALYSIS OF CALCIUM TRANSIENTS IN SKELETAL MUSCLE FIBERS. Marino Di Franco, Deida Compagnon, and Julio Vergara, Department of Physiology, UCLA, Los Angeles, CA 90024.

Single skeletal muscle fibers were mounted in a triple vaseline gap chamber and cut in an internal solution containing 10-100 μM of the Ca indicating dyes rhod-2 and fluo-3. The experimental chamber was mounted on the stage of a microscope with an epi-fluorescence attachment. The light source was a 100W tungsten/halogen lamp, and the filter combinations used (excitation/dichroic/barrier) were 490/510/520 and 546/580/590 for fluo-3 and rhod-2 respectively. The image of the muscle fiber, formed by a 20x objective, was projected on a 2-D image device of a B/W CCD camera or a photodiode. Sequences of fluorescence images were synchronized with the stimulus pulse, detected with the CCD camera at 60 fields/s, and stored in a VCR or an OMDR. The changes in fluorescence intensity elicited by action potential stimulation of isometrically contracting muscle fibers were primarily due to changes in $[Ca^{2+}]_i$ rather than to movement artifacts. The magnitude and time course of the fluorescence changes, monitored with the image detection method, matched those obtained from the fluorescence transients, recorded at 5 KHz with the photodiode. Resting calcium images showed that the nuclei of the muscle fibers fluoresced more intensely than the myoplasm. Nevertheless, at the peak of the Ca^{2+} transients (occurring between 17 and 33 ms at 10 °C), the average myoplasmic fluorescence increased to a level at which topological heterogeneities were less noticeable. The maximal dye fluorescence, needed to calculate the $[Ca^{2+}]_i$, was obtained *in situ* at the end of each experiment by fixing the fiber with Ringer + 20 mM glutaraldehyde, and subsequently exposing it to a solution containing 10 mg/ml saponin and 125 mM $CaCl_2$. (Supported by grants from MDA and NIH- AR25201).

M-Pos521

RYANODINE SENSITIVITY AND MULTIPLE CONDUCTANCE STATES OF THE CA RELEASE CHANNEL FROM NATIVE SR MEMBRANE. W.M Kwok and P.M Best. Dept. of Physiology and Biophysics. Univ. of Illinois, Urbana, IL 61801

Multiple conductance levels of the sr Ca channel in frog skeletal muscles were studied using the "sarcoball" preparation described by Stein and Palade (B.J. 54,1988). Single channel recordings of inside-out patches were made in 50 mM Ca-gluconate, 70 mM TEA-glutamate and 5 mM MOPS (pH=7.2). In addition the pipette solution contained 2 mM $MgSO_4$ and 1 mM Na_2ATP. With Ca as the charge carrier, four distinct conductance levels of 31±3, 49±2, 81±2, and 128±7 pS were observed (x±s.e.m., n=9 patches). The 49 and 81 pS levels were the dominating states with open probabilites (P_o) of .50 and .27 at -10 mV. The 31 and 128 pS states were less frequent. Multiple states were also observed with pCa=7.4 in the pipette. The channel was sensitive to ryanodine. At -20 mV, the addition of 1 μM and 10 μM ryanodine to the bath solution increased the P_o from 0.11 to 0.67 and from 0.26 to 0.99. The sensitivity of the channel to ryanodine establishes it as the ryanodine receptor protein and the four observed conductance states maybe a manifestation of the tetrameric structure of the receptor complex. Supported by NIH AR32062.

M-Pos522

Ca REUPTAKE LIMITS REPRIMING FOLLOWING CONTRACTURE. B.A. CURTIS, University of Illinois College of Medicine at Peoria, Peoria, IL 61656

The time course of both Ca reuptake and repriming were determined in bundles of 4-6 frog fast twitch fibers from tibialis anterior at 12°C. Repriming is described by a single exponential (100% repriming) with t_c= 39 sec. Following repolarization, bundles were exposed to ^{45}Ca for varying lengths of time. ^{45}Ca uptake increased with exposure time during repriming and reached a maximum of 4.2 pMCa/fiber above resting Ca influx at 3 min of exposure. The ^{45}Ca uptake data are adequately described by a time constant of 40 sec. I conclude that Ca refilling and recovery of contractile ability have the same time course. ^{45}Ca applied during repriming leaves the fiber with a time constant of 17.3 ± 1.5 min. This Ca compartment has previously been identified with the wall of the transverse tubular system. I conclude that the repriming reaction in fast skeletal muscle is limited by refilling of a Ca store in the transverse tubular system presumably emptied to initiate the preceding contracture. Supported by the Illinois Affiliate, American Heart Association.

M-Pos523

IMMUNOCYTOCHEMICAL LOCALIZATION OF ALPHA & BETA AVIAN SKELETAL MUSCLE FOOT PROTEINS. T. Deerinck, M. Ellisman, C.F. Beck*, J.A. Nichol+ & J.L. Sutko+. Dept. Neuroscience, Univ. California, San Diego; *Dept. Biochemistry, Univ. Idaho; +Dept. Pharmacology, Univ. Nevada, Reno, Nevada.

Alpha and beta foot proteins have been localized in chicken breast muscle by both light and electron microscopic immunolabeling techniques. From immunofluorescent microscopy of longitudinal sections, both alpha and beta proteins exhibit an identical, repetitive punctate distribution near the Z-lines. In serial cross sections, both proteins have similar distributions in the same fibers. Both proteins are associated with the terminal cisternae of the sarcoplasmic reticulum by immunoelectron microscopy. The localization of these proteins to the triadic junction, their large size and ability to bind (^3H)ryanodine are consistent with their identification as foot proteins. These data suggest that the foot proteins coexist in the same triad junction and indicate a previously unappreciated level of biochemical, structural and functional complexity for the triad junction. (Supported by NIH HL27470, NS14718, NS26739, RR04050; NSF DCB8819423, DCB8811-713 and AHA).

M-Pos524

DIHYDROPIRINE DERIVATIVES DO NOT BLOCK THE INOSITOL (1,4,5) TRISPHOSPHATE EFFECTS ON $[Ca^{2+}]_i$ IN SKELETAL MUSCLE. J.R. López, IVIC, Caracas, Venezuela.

We have measured the intracellular Ca^{2+} concentration ($[Ca^{2+}]_i$) by means of Ca^{2+} selective microelectrodes in quiescent intact fibers isolated from Leptodactylus insularis, microinjected with InsP3 (0.5μM) before and after the muscle bundles were incubated in nitrendipine, or nifedipine. The $[Ca^{2+}]_i$ in muscle fibers was 0.12 ± 0.01μM (M ± SEM, n=13) and the microinjection of InsP3 (0.5μM) induced a transient increment in the $[Ca^{2+}]_i$ reaching a peak value of 0.63 ± 0.02μM (n=10). The incubation of the muscle bundles in either nitrendipine (200μM) or nifedipine (200μ) for 10 minutes prior to the microinjection did not modify the InsP3 effect on the transient increment in $[Ca]_i$. The $[Ca]_i$ after the InsP3 microinjection in the presence of nitrendipine was 0.58 ± 0.02μM (n=12) and 0.69 ± 0.03μM (n=9) when nifedipine was added. These results suggest that the transient elevation in the $[Ca^{2+}]_i$ was due to a release of Ca^{2+} from intracellular store, and not by an activation of the dihydropirine calcium channels. (Supported by Angelini Pharmaceuticals and NIH).

M-Pos525

EFFECTS OF INOSITOL 1,4,5 TRISPHOSPHATE ON MYOPLASMIC $[Ca^{2+}]_i$ IN SKELETAL MUSCLE. J.R. López, L. Parra. CBB. IVIC, Caracas.

We have measured the myoplasmic free calcium concentration ($[Ca^{2+}]_i$) by means of calcium selective microelectrodes in intact fibers isolated from Leptodactylus insularis microinjected with InsP3. In muscle fibers bathed in normal Ringer the mean resting $[Ca^{2+}]_i$ was 0.11 ± 0.01 mM (M ± SEM n=20). The microinjection of InsP3 (0.5 and 1 uM) induced transient increments in the $[Ca^{2+}]_i$ to 0.53 ± 0.03 uM (n=11) and 0.94 ± 0.06μM (n=10) respectively. The exposure of a muscle to 10 mM KCl, produced a partial depolarization associated with a slow increase in $[Ca^{2+}]_i$ to 0.38 ± 0.06 (n=8). The microinjection of InsP3 (0.5 and 1 uM) in these partially depolarized muscle fibers induced transients enhancements of the resting $[Ca^{2+}]_i$ that were greater than the increase observed in the normally polarized muscle. These data support the hypothesis that InsP3 could play an important role as an intracellular messenger involved in the calcium release process in skeletal muscle, and suggest that its effect on Ca^{2+} release might be regulated by the membrane potential. (Supported by Angelini Pharmaceuticals).

M-Pos526

EFFECTS OF 2, 3-BUTANEDIONE-MONOXIME ON $[Ca^{2+}]_i$ AND MYOFILAMENT RESPONSIVENESS. Judith K. Gwathmey, Harvard Medical School, Boston, MA, and R. John Solaro. Unversity of Illinois. Chicago, Ill.

2, 3-Butanedione-monoxime (BDM) is a negative inotropic agent with proposed mechanisms of action on membrane Ca^{2+} currents, action potential parameters (APP), myofilament Ca^{2+} sensitivity and/or crossbridge kinetics. We investigated the effect of 3 mM BDM on these parameters. Membrane Ca^{2+} currents were reduced by 7.9±1% (n=11;p< .01) with no significant change in APP. $[Ca^{2+}]_i$ transient peak amplitude was reduced in aequorin-loaded papillary muscles (n=5) and in fura-2 loaded voltage-clamped isolated myocytes (n=5). BDM shifted steady-state force-Ca^{2+} relationship to the right (.1±0 pCa units;p<.01) with reduction in the Hill coefficient (1.64±.2 units; p<.01) and F_{max} (40±5%; p<.01). Ca^{2+} binding to TNC in skinned fiber preparations from beef heart revealed no difference in affinity or stoichiometry of Ca^{2+} binding in the presence of 2 or 10 mM BDM. These data suggest that BDM acts by: 1) reducing membrane Ca^{2+} currents; 2) reducing SR Ca^{2+} release; and 3) altering cross-bridge kinetics through effects on actin-myosin interaction resulting in shift to higher pCa and reduced F_{max}.

M-Pos527

DIFFERENTIAL BLOCKAGE OF Q_β AND Q_γ BY NIFEDIPINE IN FROG CUT TWITCH FIBERS. Wei Chen and Chiu Shuen Hui, Department of Physiol. and Biophys., Indiana University Medical Center, Indianapolis, IN 46223.

Charge movement was measured from cut fibers of R. temporaria using the double vaseline-gap voltage clamp (Hui & Chandler, Biophys. J. 53: 646a, 1988). The effect of nifedipine on Q_β and Q_γ was studied by comparing the components separated from the steady-state Q-V plots before and after the application of the drug. The blocking effect of nifedipine is more enhanced at H.P. -70 mV than at -90 mV. At -70 mV, low concentrations (20-100 nM) of nifedipine blocks Q_β more effectively than Q_γ. At higher concentrations, Q_γ is completely blocked whereas Q_β is only partially blocked as if some Q_β is nifedipine-resistant, although a concentration higher than 2 μM has not been used. Specifically, the half blocking concentration of nifedipine at -70 mV is about 13 nM for Q_β and 120 nM for Q_γ. This suggests that Q_β and Q_γ could be located in different macromolecules or subunits which have different binding affinities for nifedipine. The results also rule out the possibility that Q_β triggers Ca release which, in turn, triggers the movement of Q_γ. (Supported by NIH NS-21955 and a grant from MDA).

M-Pos528

EFFECTS OF CAFFEINE, RYANODINE, BAY K 8644, AND D-600 ON PROPAGATED CONTRACTIONS IN RAT CARDIAC MUSCLE

Marcel C.G. Daniels and Henk E.D.J. ter Keurs. University of Calgary, Calgary, Canada.

Propagating contractions (PC) may be triggered in the damaged ends of ventricular trabeculae (T) upon relaxation of electrically stimulated twitches. Propagation velocity (mm/s;Vp) varies between .5 and 15. We analyzed the contribution of sarcoplasmic reticular (SR) and cytosolic calcium levels to triggering and propagation of PC. PC were induced in T superfused with Krebs-Henseleit at varied $[Ca^{++}]_o$ at 20±1 C, and stimulated at 2Hz with trains, separated by 15s intervals. Force was measured with a strain gauge, and sarcomere length with laser diffraction techniques at multiple sites of T. Caffeine and ryanodine decreased twitch force (Ft) and prolonged relaxation, thereby increasing force at which PC started (Fr); time to peak force of PC (dtFpc) decreased, and Vp increased (see table). In contrast, calcium channel modulating drugs (D-600 and Bay K 8644) did not affect diastolic force; dtFpc decreased and Vp increased only when Ft increased. For all drugs, force of PC (Fpc) increased with increasing Vp, but decreased with decreasing Ft. It is concluded that triggering of PC is facilitated (ie dtFpc is decreased) and Vp is increased by increased calcium levels in both SR (as reflected by Ft) and cytosol (increased Fr). Furthermore, Fpc increases with Vp due to simultaneous activation of more cells along T, unless the SR is depleted of calcium.

	n	Ft	dtFpc	Fpc	Vp
caffeine 0.3 mM	5	79±6	49±10	252±122	322±22
caffeine 1.0 mM	10	50±7	49±5	81±36	839±104
ryanodine 100 nM	7	69±12	70±3	21±6	168±10
ryanodine 30 nM	6	81±4	85±1	136±25	298±37
Bay K 8644 5 nM	7	132±5	65±3	476±33	406±20
D-600 100 nM	8	79±3	124±3	49±2	84±4

values expressed as % of control±sem

M-Pos529

ANTI-RYANODINE RECEPTOR ANTIBODIES AS PROBES FOR LIGAND GATING OF SINGLE SR CALCIUM RELEASE CHANNELS.

Fill, M., R. Mejia-Alvarez, P. Volpe, F. Zorzato, and E. Stefani. Baylor Col. Med., Houston, TX, Univ. Texas Med. Branch, Galveston, TX, and Univ. Toronto, Canada.

Single sarcoplasmic reticulum (SR) calcium release channels from rabbit skeletal muscle were reconstituted in lipid planar bilayers (5:3:2, POPE:POPS:POPC, 50 mg/ml decane). Solutions contained (mM, microsomes cis): 250 cis & 50 trans Cs-CH_3SO_3, 10 Cs-HEPES (pH 7.4), pCa = 5. A large conductance (gCs 480 pS) was pharmacologically identified as the SR release channel. Polyclonal anti-ryanodine receptor antibodies (Ab), Ab/SR protein ratios from 0.5 to 2, were added to the cis chamber. Antibody decreased single channel open probability (0.12 to less than 0.01). Addition of calcium (pCa = 4) did not alter Ab action. Addition of ATP (2 mM) reversed Ab action. After ATP reversal, the conductance, gating properties, and Po in the presence of Ab were comparable to controls. Localization of the antigenic regions reveal that these regions contain a putative calcium binding site. Our results support the suggestion that the antibodies interact with regions of the ryanodine receptor which mediate the Ca induced Ca release mechanism. Further, ATP activation and the Ca induced Ca release mechanism appear to operate independently. Supported by NIH and MDA.

M-Pos530

CLONING OF RYANODINE RECEPTOR COMPLEMENTARY DNA FROM SKELETAL AND CARDIAC MUSCLE.

F.A. Lai, J.K. LaDine and G. Meissner. Dept. of Biochemistry, University of North Carolina, Chapel Hill, NC 27599.

Skeletal and cardiac ryanodine receptors have been purified and comprise high M_r polypeptides (Lai *et al*, Nature 331, 315, 1988; Anderson *et al*, *JBC* 264, 1329, 1989). A rabbit skeletal muscle λgt11 cDNA library was screened with affinity purified rabbit anti-rat ryanodine receptor antibodies. Several clones were identified whose inserts encompassed ~5 kb of the ~15 kb ryanodine receptor sequence reported by Takeshima *et al* (*Nature* 339, 439, 1989). The clone most strongly reactive with the antibodies encoded the C-terminal one eighth of the protein, which is believed to include the membrane-spanning segments of the receptor. Due to the structural similarity in skeletal and cardiac ryanodine receptors, we have used our skeletal receptor cDNAs as probes to screen a rat cardiac muscle λgt11 cDNA library at low stringency in an attempt to isolate cardiac ryanodine receptor cDNA clones. Several "positives" were identified and are currently being characterized. Supported by NIH and MDA.

M-Pos531

TETRACAINE INHIBITION OF THE CA^{2+} RELEASE CHANNEL FROM SKELETAL SARCOPLASMIC RETICULUM.

L. Xu, R.V. Jones, and G. Meissner. (Intro. by Arthur L. Finn) Dept. of Biochemistry, Univ. of North Carolina, Chapel Hill, NC 27599-7260.

Vesicle- $^{45}Ca^{2+}$ flux and single channel recordings of K^+ currents of the purified channel complex showed that the Ca^{2+}- and ATP-gated Ca^{2+} release channel of skeletal muscle sarcoplasmic reticulum is inhibited by tetracaine. The single channel measurements revealed that tetracaine, added to either the cis or trans side of the bilayer, inhibited Ca^{2+} release by decreasing channel open time without changing the unit conductance. Tetracaine concentrations of > 1 mM were required to fully inhibit the Ca^{2+}-gated release channel. At 500 μM, tetracaine inhibition was characterized by prolonged closed intervals interrupted by bursts of rapid channel openings and closings. Inhibition by tetracaine was voltage-dependent and independent of Ca^{2+} concentration and the presence of ATP. Supported by NIH.

M-Pos532

HIGH AFFINITY RYANODINE AND PN200-110 BINDING TO RABBIT SKELETAL MUSCLE TRIADS.

K. Anderson, R. Grunwald, A. El-Hashem, R. Sealock*, and G. Meissner. Depts. of Biochemistry and Physiology*, Univ. of North Carolina, Chapel Hill, NC 27599.

Rabbit skeletal muscle junctional T-tubule sarcoplasmic reticulum complexes (triads) were isolated on isopycnic sucrose density gradients using a modification of the pyrophosphate procedure of Mitchell *et al.* (*JCB* 96, 1017, 1983). Triads were identified by thin-section electron microscopy and by the comigration of [^{3}H]PN200-110 and [^{3}H]ryanodine binding activities with high affinity B_{max} values of ~5-20 and ~3-10 pmol/mg protein, respectively. These B_{max} values correspond to a PN200-110/ryanodine binding ratio of 1.5-2.0. Assuming one ligand site per receptor, this ratio agrees with recent structural predictions of dihydropyridine (DHP)/ryanodine receptor stoichiometry (Block *et al.*, *JCB* 107, 1587, 1988). The DHP receptor agonist, nifedipine (≤1 μM), did not affect [^{3}H]ryanodine binding. In contrast, [^{3}H]PN200-110 binding increased in the presence of 10-100 μM ryanodine and decreased at ≥1 mM ryanodine. This suggests a possible interaction between the Ca^{+2} release channel and the DHP receptor. Supported by NIH.

M-Pos533

DOES THE INCREASE IN K^+ EFFLUX FOLLOWING FATIGUE INHIBIT TETANIC FORCE RECOVERY? J.M. Renaud. Dept. of Biological Sciences, Univ. of Calgary, Alberta, Canada T2N-1N4.

There is now evidence that the extracellular H^+ inhibits P_o (tetanic force) recovery in frog sartorius muscles (Renaud, J. Physiol. 416:31, 1989). During fatigue development the K^+ efflux rate increases and is higher at acidic pH_o than at alkaline pH_o (Mainwood and Lucier, Can. J. Physiol. Pharmac. 50:132, 1972). The effect of an increase K^+ concentration on P_o of frog sartorius muscles was studied. When the K^+ concentration is raised from 3 to 10 mM, P_o of unfatigued muscles decreases by less than 20%. However, a similar increase in K^+ following fatigue reduces significantly the recovery P_o, both in rate and magnitude. Furthermore, the K^+ effect is greater at pH_o 6.4 than at 7.2. It is proposed that the slow recovery of P_o at acidic pH_o is in part due to the larger K^+ efflux causing a K^+ accumulation near the membrane.

M-Pos534

PERFUSING PATCH PIPETTES QUIETLY AND EASILY. J.M. Tang, J. Wang, F.N. Quandt and R.S. Eisenberg. Dept. of Physiology, Rush Medical College, Chicago IL 60612.

We describe a simple method to change the fluid in a patch pipette that introduces little excess noise, requires only minor modification of standard equipment and procedures, does not damage gigaseal or channels, and so may be generally useful. The key to the system is the polyimide coated quartz capillary used to make the perfusion pipette that fits within the patch pipette. The capillary is pulled to an inside diameter of ~35 μm and yet is strong enough to survive through many experiments. One end of the capillary is positioned close to the tip of the patch pipette, where it fills some half of the cross section. The other end of the capillary is connected to polyethylene (PE) tubing that is inserted into the pipette holder through a hole and grease seal. The far end of the PE tubing is placed in perfusion fluid. Perfusion is driven by servo controlled suction through the vacuum line of the pipette holder. Measurements of the reversal potential of a Ca^{2+} activated K^+ channel in neuroblastoma cells show that perfusion is complete in ~60 seconds. Measurements of the power spectrum show only a small increase of noise at frequencies below a few kilohertz.

M-Pos535

CONTRACTURES AND RELOADING IN SKINNED LOBSTER MUSCLE FIBERS. J.M. Tang, J. Wang, T. Lea* and R.S. Eisenberg. Dept. of Physiology, Rush Medical College, Chicago IL 60612 and *University Laboratory of Physiology, Oxford University, England.

Skinned fibers from the lobster remotor muscle are interesting because single K^+ and Ca^{2+} channels of its sarcoplasmic reticulum (SR) can be studied by "On-SR" recording using the patch clamp technique (Tang et al., J. Gen. Physiol. 94:261, 1989; Wang et al., Biophys. J. 55:207a, 1989). In 13 experiments, 20 mM caffeine produces ~10 kN/m^2 tension, which is comparable to other muscles, given that ~70% of the skinned fiber is SR. Immediately following the caffeine contracture, the fiber is unable to contract, presumably because the SR is depleted of Ca^{2+}. But after 10 minutes of recovery in a loading solution containing 160 nM free Ca^{2+}, the fiber gives a second caffeine contracture, presumably because the SR refills with Ca^{2+} during recovery. The recovered contracture is ~70% of the first, in 4 experiments completed to date, but reloading for 20 minutes does not increase its size. Cycles of contracture and reloading produced only a gradual diminution of contracture tension.

The skinned lobster remotor fiber seems as viable as most skinned preparations.

M-Pos536

PLASMALEMMAL VOLTAGE MODULATES THE EFFECT OF CAFFEINE IN INACTIVATED SKELETAL MUSCLE FIBERS. Esther M. Gallant, Dept. of Veterinary Biology, Univ. of Minnesota, St. Paul, MN 55108.

This study investigated whether calcium release initiated by caffeine, which acts directly on the sarcoplasmic reticulum (SR), is graded with plasmalemmal resting voltage. Small bundles of intact skeletal muscle cells were dissected from porcine limb muscles. Caffeine contractures (10mM) were maximal in muscles which were slightly depolarized (15-30 mM K^+). Depolarization for 5 min with 30 mM K^+, which inactivates the fibers, increased the magnitude of the caffeine contractures 2-3 fold and shifted the contracture threshold to lower caffeine concentrations. Thus, contractures elicited by direct action of caffeine on the SR were graded by plasmalemmal resting voltage. This suggests that plasmalemmal voltage, independent of excitation-contraction coupling, modulates SR Ca^{2+} release, and agrees with previous studies in which resting transverse-tubule or sarcolemmal voltage modulated SR Ca^{2+} release in skinned or intact fibers, respectively (Pflugers Arch.:Donaldson et al., 414:15; Gallant & Donaldson, 414:24, 1989).

M-Pos537

RYANODINE INDUCES A CONFORMATIONAL CHANGE IN THE SARCOPLASMIC RETICULUM Ca RELEASE CHANNEL. **Jianjie Ma, Kevin P. Campbell, and Roberto Coronado.** Department of Physiology, Rush Medical College, Chicago, IL; University of Iowa, Iowa City, Iowa; University of Wisconsin, Madison, WI.

The SR Ca release channel in skeletal muscle is a homotetramer structure of the 450 kD ryanodine receptor. Ryanodine changes the kinetics of the release channel gating from fast to slow and locks the channel into a long-lived open state. In the presence of 200 nM ryanodine: 1) Open lifetime of the channel was increased from 0.6 ms to 10 ms, whereas, closed lifetime constants were not affected; 2) Kinetics of the channel remained the same in a wide range of Ca from 50 nM to 3 mM, thereby Ca dependent gating was lost; 3) Open probability vs pH curve showed a pronounced hysteresis. Titration in the acidic direction resulted in a pK of 6.2, in the alkaline direction pK was larger than 9. In channels in the absence of ryanodine, pK of proton site involved in channel gating was 7.1. These data suggest that there is a significant conformational change in the Ca release channel upon binding of ryanodine.

M-Pos538

HIGH RECEPTOR OCCUPANCY IN RENAL ARTERY INCREASES INOSITOL PHOSPHATE (IP) PRODUCTION AND DECREASES THE ABILITY OF NIFEDIPINE TO INHIBIT STRESS (S). P. H. Ratz, J. Weiseman, and A. Boothe. Eastern Virginia Medical School, Norfolk, VA 23501

In some smooth muscles, the effectiveness of Ca^{2+} channel blockers (CB) to inhibit S is dependent on the α receptor agonist concentration. The cellular basis for this phenomenon was studied. Maximum (EC_{100}; 1E-7 M) and supramaximum ($EC_{>100}$; > 1E-7 M) PhE produced similar steady-state levels of S (about 1.0 fold optimum S) and crossbridge phosphorylation (about 34%). However, the production of IP by EC_{100} and $EC_{>100}$ PhE differed dramatically (fold increase above basal was 1.65, 3.08, 8.98 and 9.6 for 1E-7, -6, -4, and -3 M, respectively). Likewise, S produced by EC_{100} PhE was much more effectively inhibited by CB than S produced by $EC_{>100}$ PhE. A causal relationship between IP production and CB inhibitory efficacy is implied. Support: AHA & VA Affiliate, Jeffress, and PMAF.

M-Pos539

EFFECTS OF CALCIUM AND ISOPROTERENOL ON AEQUORIN SIGNALS FROM ISOLATED MAMMALIAN CARDIAC MYOCYTES. Arthur J. Meuse, Cynthia L. Perreault, and James P. Morgan, Department of Medicine, Harvard Medical School, Boston, MA 02215

Aequorin (AEQ) has been successfully used for the detection of intracellular calcium signals ($[Ca^{2+}]_i$) in various preparations: whole heart, isolated muscle and enzymatically isolated single cells. High yields (50-80%) of isolated, aequorin-loaded cardiac myocytes were obtained using a macroinjection and enzymatic digestion technique previously described (Meuse, et al. 1989. J. Gen. Physiol. 94:22a). Subpopulations of cells isolated in this manner were subjected to varying extracellular calcium concentrations as well as doses of isoproterenol. Electrical stimulation of fields of 50-200 cells revealed an increase in $[Ca^{2+}]_i$ in the high Ca^{2+} and isoproterenol treated preparations. Percent cell shortening obtained from video recordings of the cells was employed as an index of contractility. The configuration, time course and pharmacological response of the Ca^{2+} signal at 30°C were similar to those recorded with AEQ from whole heart and isolated muscle studies.

M-Pos540

BEAT-TO-BEAT RECORDING OF INTRACELLULAR CALCIUM WITH AEQUORIN IN THE BLOOD-PERFUSED DOG HEART.

Marc J. Levine, M.D., Arthur J. Meuse, Ph.D., Jun Watanabe, M.D., Lisa A. Bentivegna, B.A., Robert G. Johnson, M.D., William Grossman, M.D., and James P. Morgan, M.D., Ph.D. Harvard-Thorndike Laboratory, Beth Israel Hospital, Boston, MA.

The bioluminescent indicator aequorin (AEQ) has been used to record intracellular calcium signals ($[Ca]_i$) in the isolated, buffer-perfused ferret heart. We have now been able to extend this technique to the isolated, blood-perfused dog heart. This model has the advantage of large size and the potential for recording $[Ca]_i$ during blood perfusion. AEQ was loaded into the myocytes of a small area of LV subepicardium in 8 dog hearts. Simultaneous ECG, LV pressure (LVP), perfusion pressure, and AEQ-generated light signal were recorded. Under buffer perfusion at 30° C, $[Ca]_i$ showed a variation between systolic and diastolic levels on a beat-to-beat basis. Signal-averaging was not required. Conversion from buffer to blood perfusion did not interfere with the recording of $[Ca]_i$. Systolic $[Ca]_i$ reached its peak before the development of peak LVP. Diastolic $[Ca]_i$ returned to baseline before LVP returned to baseline. $[Ca]_i$ could be modulated through pharmacologic intervention: increasing the perfusate calcium increased the amplitude of the systolic $[Ca]_i$, as did the addition of isoproterenol. $[Ca]_i$ also increased during transient global ischemia, returning to baseline values upon reperfusion.

This is the first report of intracellular calcium recording in an isolated, blood perfused large mammalian heart.

M-Pos541

PHENYLEPHRINE-INDUCED CONTRACTION OF SINGLE SKINNED SMOOTH MUSCLE CELLS AT RESTING $[Ca^{2+}]_i$.

EM Collins. KG Morgan. Department of Medicine. Harvard Medical School. Boston, MA 02215.

Freshly enzymatically isolated single ferret aorta smooth muscle cells were prepared in a collagenase, elastase and trypsin inhibitor solution. The cells were attached to a force transducer as previously described. The cell membrane was made hyperpermeable by exposure to 30 mcg/ml of saponin for 15 minutes. Maximal force (552±29 mcg) was obtained at a pCa of 6.0. At a pCa of 7.0 the addition of phenylephrine resulted in a contraction (103±31 mcg) of the cells which was reversed by phentolamine. We have previously determined resting $[Ca]_i$ in ferret aorta cells to be a pCa of 6.5-6.7. These results indicate: 1) these skinned cells retain receptor function; and 2) phenylephrine increases the apparent calcium sensitivity of the contractile apparatus. This should be a useful preparation for future studies on mechanisms of contraction in vascular smooth muscle. Support: NIH HL42293.

M-Pos542

A METHOD FOR CALCULATING CALCIUM RELEASE FROM THE SARCOPLASMIC RETICULUM OF CARDIAC MYOCYTES

Karin R.Sipido and W.Gil Wier
Department of Physiology, University of Maryland, Baltimore MD 21201

Calcium (Ca^{2+}) release from the sarcoplasmic reticulum (s.r.) during excitation-contraction coupling was calculated from the cytoplasmic free $[Ca^{2+}]_i$ transient, as measured with fura-2 in guinea pig ventricular myocytes (23°C).

The flux of Ca^{2+} from the s.r. was obtained after subtracting all other known Ca^{2+} fluxes from the rate of change of the free $[Ca^{2+}]_i$ transient. Fura-2 signals were corrected for kinetic lags. Na/Ca exchange was eliminated by the use of Na free solutions inside and outside the cell. The flux through the L-type Ca^{2+} channel was calculated from the verapamil sensitive current. The conductance of the Ca^{2+} leak across the sarcolemma (s.l.) and the characteristics of the s.l. Ca^{2+} pump were determined from the decay of the free $[Ca^{2+}]_i$ transient in the presence of caffeine (10mM) to inhibit s.r. Ca^{2+} release and uptake. The intracellular Ca^{2+} binding was estimated from the rise of the free $[Ca^{2+}]_i$ transient in the presence of caffeine. Parameters for the s.r. Ca^{2+} pump were taken from the literature and adjusted to match the basal s.r. Ca^{2+} leak as calculated from data on rest decay.

The peak s.r. release rate (5 to 10mmoles/liter/s) was reached within 20ms after depolarization to +10mV and almost completely inactivated after 50ms. A small remaining component was slowly inactivated, without distinct turn-off on repolarization.

M-Pos543

CHANGES IN $[Ca^{2+}]_i$ PRODUCED BY MICROINJECTION OF INOSITOL (1,4,5) TRISPHOSPHATE IN SWINE SKELETAL MUSCLE.

J.R. López, N. Linares, CBB, IVIC, Caracas, Venezuela.

We have measured the intracellular Ca^{2+} concentration ($[Ca]_i$) by means of calcium selective microelectrodes, in intact external intercostal muscle fibers isolated from control and malignant hyperthermia (MH) susceptible swine. Determinations of $[Ca^{2+}]_i$ were carried out before and after the muscle fibers were microinjected with InsP3 (0.5μM). In control fibers the $[Ca]_i$ was 0.13 ± 0.01μM (M ± SEM, n=10) while it was 0.31 ± 0.02μM (n=14) in the MH susceptible muscle. The microinjection of InsP3 (0.5μM) induced a transients elevation in the $[Ca]_i$ which were more pronounced in the MH (0.91 ± 0.04μM, n=9) than in control muscle fibers (0.43 ± 0.03μM, n=11). These results support the hypothesis the InsP3 is involved in the regulation of calcium release from intracellular store in swine skeletal muscle and that there is an abnormality in the InsP3 receptor and/or that the activation of the calcium channel in response to InsP3 depend on the free $[Ca^{2+}]_i$. (Supported by CONICIT S1-1277 and Angelini Pharmaceuticals).

M-Pos544

CHLORPROMAZINE CHANGE RESTING $[Ca^{2+}]_i$ IN AMPHIBIAN SKELETAL MUSCLE. [1]J.R. López, [1]L. Parra, [1]V. Sánchez, [2]P. Allen. [1]CBB, IVIC, Caracas, Venezuela. [2]Anesthesia Department Brigham Women's Hospital, Boston, MA.

We have studied the effects of chlorpromazine (C) on intracellular free Ca^{2+} concentration ($[Ca^{2+}]_i$) by means of Ca^{2+} selective microelectrodes in muscle fibers isolated from Leptodactylus insularis. From a resting value of 0.10 ± 0.01 μM (M ± SEM, n=16), was increased to 0.37 ± 0.02 μM (n=10), to 0.61 ± 0.03 μM (n=11) and 0.76 ± 0.04 μM (n=12), in the presence of C 10^{-8}, 10^{-7} and 10^{-6} M respectively. The $[Ca^{2+}]_i$ was 6.89 ± 035 μM (n=8), and 8.53 ± 056μM (n=9) in the presence of C 10^{-5} and 10^{-4} M respectively which was associated to muscle contracture. The addition of dantrolene (10^{-5} M) blocked the increment in $[Ca^{2+}]_i$ as well as the muscle contracture. These results show that C induced increment in the $[Ca^{2+}]_i$ in a dose dependent manner. The fact that dantrolene was able to prevent the C effects, suggest that C acts probably on the sarcoplasmic reticulum (SR), since dantrolene inhibit Ca^{2+} release from the SR, without any effects on calcium influx from the extracellular space. (Supported by Sigmatau Pharmaceuticals and NIH).

M-Pos545

HALOPERIDOL INDUCES CHANGES IN $[Ca^{2+}]_i$ WITH NO EFFECTS ON CHARGE MOVEMENT. [1]J.R. López, [1]P. Bolaños, [1]González, A. [2]P. Allen [1]C. Caputo [1]CBB, IVIC, Caracas, Venezuela. [2]Dept. Anesthesia, Brigham Women's Hospital, Boston, MA.

We have studied the effect of the neuroleptic agent Haloperidol i) on $[Ca^{2+}]_i$ by means of calcium selective microelectrode and ii) on intramembrane charge movement using the triple vaseline gap voltage clamp technique in muscle fibers isolated from the Leptodactylus Insularis. The addition of haloperidol to the external solution (10^{-8}-10^{-4} M) produced an increase in the $[Ca^{2+}]_i$ which was related to drug concentration. From a control value of 0.12 ± 0.01 μM (M ± SEM, n=18), the $[Ca^{2+}]_i$ was changed to 0.26 ± 0.02 μM (10^{-8}M), 0.34 ± 0.03 μM (10^{-7}M), 0.40 ± 0.03 μM (10^{-6}M), 0.86 ± 0.03μM (10^{-5}M) and 2.63 ± 0.06 μM (10^{-4}M). The addition of dantrolene (10^{-6}M) blocked the haloperidol effects on $[Ca^{2+}]_i$. Measurements of charge 1 and 2 showed not changes in the presence of haloperidol (10^{-8}-10^{-4}) (Supported by MDA, CONICIT S1-1148 and Angelini Pharmaceuticals).

M-Pos546

MYOPLASMIC $[Ca^{2+}]$ IN SWINE SKELETAL MYOBALLS. [1]J.R. López, [2]S.R. Taylor. [1]CBB, IVIC, Caracas, Venezuela. [2]Pharmacology Department, Mayo Foundation, Rochester, MN.

We have measured the myoplasmic free calcium concentration ($[Ca^{2+}]_i$) in contracting myoballs regenerated from minced control and malignant hyperthermia (MH) susceptible skeletal muscle. The resting $[Ca^{2+}]_i$ in quiescent control myoballs was 0.13 ± 0.01μM (M ± SEM, n=18), while it was 0.22 ± 0.02μM (n=18) in the MH susceptible myoballs. Caffeine (2mM) induced an increase in the $[Ca^{2+}]_i$ which was greater in the MH (0.68 ± 0.03μM, n=15) than in control myoballs (0.30 ± 0.02μM, n=13). The addition of nitrendipine (100μM) prior to the caffeine solution did not modify the enhancement in $[Ca]_i$. Similar results were obtained in low calcium solution (0 $CaCl_2$, 3 $MgCl_2$, 3 EGTA). The incubation in subthreshold K^+ (10mM) produced a depolarization which was accompanied by an increase in the $[Ca]_i$ which were larger in the MH (0.66 ± 0.04μM, n=16) than in control (0.25 ± 0.03μM, n=10). Trasmision Electron microscopy studies performed after the experiments showed the presence of sarcomeres, in which was posible to identify contractile filaments. (Supported by Angelini Pharmaceuticals, NSF DMB 85967345).

M-Pos547

ISOPROTERENOL EFFECTS IN ADULT CANINE VENTRICULAR MYOCYTES. Q Li, CM Hohl, B Hu, RH Fertel, GP Brierley, RA Altschuld, BT Stokes. Ohio State Univ, Columbus, OH.

Changes in $[Ca^{2+}]_i$ transients and cAMP in response to varied isoproterenol (ISO) were followed using single cell FURA-2 fluorescence microscopy and RIA. ISO increased the peak and shortened the duration of electrically-triggered Ca^{2+} transients at 0.5 nM and caused maximal changes at 100 nM. The EC_{50} for shortening of Ca^{2+} transients (duration at half peak) was 3.2 nM (695 ± 160 msec in control vs 262 ± 57 msec at 100 nM ISO, mean ± SD, n = 17). ISO-stimulated cAMP production measured in parallel with the single cell experiments had an EC_{50} of 50 nM with maximal increase in cAMP at 1 μM (7.8 ± 1.0 pmol/mg protein in control; 25.3 ± 5.8 in 1 μM ISO, mean ± SE, n = 5). With 10 μM IBMX, a PDE inhibitor, the ISO vs cAMP curve was sigmoidal with maximum cAMP of 76 ± 0.7 pmol/mg; that for ISO vs $t_{1/2}$ of the Ca^{2+} transient was clearly biphasic with a maximal shortening of $t_{1/2}$ at 100 nM ISO (256 ± 75 msec). The results suggest a dissociation between effects of ISO on cAMP production and free Ca^{2+} transients that may involve G-proteins or cAMP compartmentalization. (Ohio-AHA)

M-Pos548

PRIMARY AND SECONDARY EFFECTS OF 2,3-BUTANEDIONE MONOXIME ON Ca^{++} MOBILIZATION IN MAMMALIAN HEART MUSCLE. Jian-Xun Wang and Norman K. Lee (Intr. by J. R. Blinks). Dept. of Pharmacology, Mayo Foundation, Rochester MN 55905.

2,3-butanedione monoxime (BDM) strips phosphate groups from many proteins and is thought to interfere with crossbridge cycling in muscle as a result. Myofibrillar responsiveness to Ca^{++} is clearly reduced by BDM, but there is disagreement about the effects of BDM on Ca^{++} mobilization. In rat skeletal muscle BDM decreases both force development and the amplitude of the Ca^{++} transient in a dose-related manner (J. Physiol. 407:53,1988). On the other hand, it has been reported (Biophys. J. 53:605a, 1988) that in aequorin-injected ferret papillary muscles BDM up to 5 mM decreased force without affecting the aequorin signal, and we find that in the same preparation (31°C, 3s, L_{max}) BDM up to 10 mM actually increases the amplitude of the aequorin signal (max. 23% at 6 mM) while decreasing force. However, when force development has first been eliminated by hypertonicity (sucrose), or by substitution of D_2O for H_2O, all [BDM] (1-18 mM) decreased both force and the Ca^{++} transients. These results are consistent with the hypothesis that BDM has primary actions which depress Ca^{++} mobilization as well as myofibrillar responsiveness to Ca^{++} in both cardiac and skeletal muscle, but that in cardiac muscle the primary effect of low concentrations of BDM on the Ca^{++} transient may be masked or overcome by a decrease in binding of Ca^{++} to troponin C resulting from decreased crossbridge attachment. (Support: HL 12186).

M-Pos549

ELEVATION OF $[Ca^{++}]_i$ UNMASKS STRETCH-INDUCED INCREASE IN RESTING $[Ca^{++}]_i$ IN AEQUORIN-INJECTED FROG SKELETAL MUSCLE FIBERS. J. D. Hannon and L. A. Blatter (Intr. by J. D. Lechleiter). Dept. of Pharmacology, Mayo Foundation, Rochester, MN 55905.

Stretch has been reported to increase resting $[Ca^{++}]_i$ in aequorin-injected frog skeletal muscle fibers (Biochim. Biophys. Acta. 862:441,1986), possibly by causing Ca^{++} release from the sarcoplasmic reticulum (SR). However, a subsequent attempt to reproduce these results in the same experimental apparatus was unsuccessful (E.D.W. Moore, Ph.D. thesis, Univ. MN, 1986), and we find that stretch usually does not increase the resting luminescence of aequorin-injected skeletal muscle fibers of the frog (R. temporaria, t. ant.) bathed in normal physiological salt solution. A possible explanation might be that the resting $[Ca^{++}]_i$ of such fibers is usually low enough to fall on the flat part of the aequorin calibration curve (Biophys. J. 55:490a,1989). When this is true, a small stretch-induced increase in $[Ca^{++}]_i$ might be undetectable with aequorin at normal resting $[Ca^{++}]_i$. In accord with this hypothesis, we find that stretch does regularly increase light emission from aequorin-injected fibers when resting $[Ca^{++}]_i$ has been raised (with 1 mM caffeine or 12.5 mM K^+) to a level where the calibration curve for aequorin is no longer flat. The stretch-induced increase in $[Ca^{++}]_i$ is not abolished by removal of extracellular Ca^{++} or application of nifedipine (10^{-5} M), which is consistent with the hypothesis that the Ca^{++} is released from the SR. It is not yet clear why the resting $[Ca^{++}]_i$ in the initial experiments was higher than in subsequent ones. (Support: HL 12186).

M-Pos550

$[Mg^{2+}]$ DECREASES RYANODINE DEPRESSION OF TENSION TRANSIENTS IN SKINNED MUSCLE FIBERS OF THE RABBIT. JY Su, Anesthesiol, Univ of Washington, Seattle, WA 98195

In skinned muscle fibers, ryanodine has been shown to depress caffeine-induced tension transients (TT) in a subsequent Ca loading-release cycle as a function of $[Ca^{2+}]$. This study showed that $[Mg^{2+}]$ has an opposite effect, in agreement with studies of ryanodine-receptor binding in isolated SR. Fiber bundles from homogenized, skinned papillary muscle were dissected and mounted for force measurement. Calcium loading-release of the SR was performed on the fiber bundles using a releasing solution containing 25mM caffeine. In each case, the area of the resulting TT was measured. Each experiment consisted of three such cycles: a control (C_1) (no ryanodine, pMg 4.0), a test (releasing solution ± 1μM ryanodine at pMg = 3.0-4.5), and finally a second control (C_2) (no ryanodine, pMg 4.0). The TT/C2 area was expressed as a percentage of TT/C_1. Ryanodine depression of TT/C_2 increased with increasing pMg (ID_{50} ~ 3.3), again suggesting that the depression is enhanced by ryanodine binding. (Supported by NIH HL20754).

M-Pos551

MODULATION OF E-C COUPLING IN CAT MYOCARDIUM BY ENDOCARDIAL ENDOTHELIUM. Bourreau, J.-P., Banijamali, H.S., and Challice, C.E. Department of Physics, The University of Calgary, Calgary, AB, T2N 1N4, Canada.

Damaging the endocardial endothelium results in an immediate decrease in peak isometric tension, but modification of action potential appears only subsequently. The same damaging procedure applied to the epicardial surface produces no effect, indicating the above effects to be induced by selectively damaging the ventricular lining. Endocardial endothelium damage suppresses the after-contractions induced by beta-stimulation in a depolarized preparation, and also induces an increase in the amount of calcium recirculating through the SR between beats. In a medium containing 3.10^{-6} M ryanodine, selective endocardium damage fails to further modify myocardial E-C coupling. There is a similarity at the action potential level between selective damaging the endocardium and raising the extracellular calcium concentration. To explain these results a model involving the SR is presented.

M-Pos552

MAPPING PROTEASE SENSITIVE REGIONS OF THE RYANODINE RECEPTOR FROM SKELETAL MUSCLE. Andrew R. Marks, Sidney Fleischer, Bernardo Nadal-Ginard and Paul Tempst. Harvard Medical School, Boston, MA and Vanderbilt University, Nashville, TN.

The ryanodine receptor (RyRec)/calcium release channel (CRC)/junctional channel complex (JCC) has been isolated and found to be morphologically equivalent to the foot structures of terminal cisternae of sarcoplasmic reticulum (SR) and functionally to the calcium release channel (CRC) of SR. We have carried out limited proteolysis on the RyRec in CHAPS using Staph. aureus V8 endoprotease Glu-C and Achromobacter endoprotease Lys-C and amino acid sequencing of the HPLC purified peptides. Sequence analysis shows that 29 of 30 peptides (5% of sequence) map in five protease sensitive regions (PSRs) of the RyRec. One of these PSRs maps to the most hydrophilic protion of the RyRec. Two other PSRs flank a putative modulator region of the RyRec [Takeshima et al., Nature 339:439,(1989)]. S1 nuclease analysis using a cloned cDNA probe encoding a portion of the RyRec from skeletal muscle shows that the most hydrophilic portion of the RyRec is highly conserved between skeletal, cardiac and aortic smooth muscle receptors. We suggest that the five PSRs identified correspond to surface exposed regions of the RyRec. These studies provide the basis for an approach to structure-function analysis of the CRC. (NIH DK 14632, Clinician Scientist of AHA to ARM.)

M-Pos553

DISSOCIATION BETWEEN POSTEXTRASYSTOLIC POTENTIATION AND TENSION INDEPENDENT HEAT IN RABBIT PAPILLARY MUSCLES. E.M. Blanchard, N.R. Alpert. Dept. Physiol & Biophy Univ Vermont. We tested the hypothesis that post-extrasystolic potentiation and the beat-dependent decay of potentiation can be attributed to a parallel decline in the total activator calcium released and sequestered by the sarcoplasmic reticulum (SR). We measured tension independent heat (TIH) from papillary muscles (normal and pressure-overload rabbits) following short-term changes in stimulation pattern. An "extrasystole" 1 sec after a regular twitch (presys) resulted in optimal potentiation of the integral of twitch tension (TTI) for the regular twitch (post-sys) 4 sec later. The ratio of postsys/presys for TTI was 1.45 $\pm$0.07 and 1.62$\pm$0.06 for normal (n=6) and PO (n=8) muscles, respectively. Contrary to the hypothesis of parallel changes in total calcium cycling from the SR, TIH was unchanged in either muscle group following the extrasystole. In addition, while potentiation of normal muscles decayed exponentially over 5 beats, the potentiation of PO muscles decayed completely in 1 beat. These results suggest that the mechanism of "post- extrasystolic potentiation" is inadequately understood. (supported by PHS 28001)

M-Pos554

EFFECT OF TMB-8 ON SLOW CALCIUM CURRENT OF SKELETAL MUSCLE. Gamboa-Aldeco R. & Cortés-Peñaloza J.L. Universidad Juárez Autónoma de Tabasco & Hospital del Niño, Tabasco, México.

TMB-8 inhibits Ca ion dependent processes in several tissues by stabilizing intracellular stores of membrane-bound Ca. We have tested the effect of TMB-8 on the slow Ca current, recorded from mammalian twitch cut fibers with the vaseline gap technique. TMB-8 (100 uM) reduced peak amplitude of Ca current to 10 % of control(n=3, at 0 mV). This same concentration did not affected the charge movement. Dissociation of Ca current from charge movement by TMB-8, suggested that gating mechanism is not involved in the blocking mechanism of this agent on Ca current. In agreement with reported Ca antagonistic behaviour, it is proposed that TMB-8 blocks slow Ca current by inhibiting Ca release from Ca binding sites into the channel. Supported by SEP C88080211 and CONACYT P219CCOL880488, México grants.

M-Pos555

GRADED SUBTHRESHOLD Ca^{2+} RELEASE IN RAT CARDIAC MYOCYTES. H.A. Spurgeon, A. Talo, E.G. Lakatta and M.D. Stern. Gerontology Research Center, NIA, Baltimore, MD.

Sustained depolarization (-45 to 0 mV) of rat cardiac ventricular cells elicits a phasic increase in cytosolic Ca^{2+} (Ca_i), (measured by Indo-1), and a twitch contraction followed by sustained components (Fig. A). Smaller depolarizations (to -35 mV) still cause a slowly rising, graded increase in Ca_i and contraction (Fig. B). During the small depolarization, either I_{Ca} blockade (Nitrendipine, 2 µM), or sarcoplasmic reticulum (SR) Ca^{2+} depletion (Fig. C) by ryanodine (1 µM), can abolish the steady increase in Ca_i. Small depolarization thus causes stable SR Ca^{2+} release which is graded by I_{Ca}. This excludes Ca^{2+} induced Ca^{2+} release mediated via a common cytosolic Ca^{2+} pool.

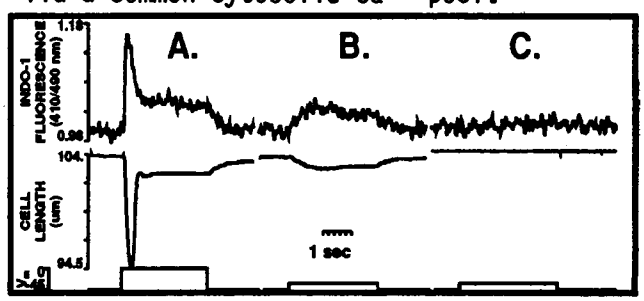

M-Pos556

DIFFERENTIAL DEPENDENCE ON PULSE DURATION OF Ca TRANSIENT AND TWITCH MAGNITUDES IN RAT VENTRICULAR MYOCYTES. W.H. duBell, H.A. Spurgeon and E.G. Lakatta Gerontology Research Center, Baltimore, MD 21224

The dependence of the steady state Ca transient (CaT) and twitch (T) magnitudes on pulse duration was determined in voltage clamped indo-1/AM loaded myocytes. Seven 100 ms pulses to 0 mV (H.P. = -40 mV) at 0.5 Hz were followed by test pulses (1 to 1000 ms). Figure shows magnitude of test CaT and T (normalized to pulse 7) vs. log test pulse duration. The PD_{50} for CaT is 7 ms vs. 11 ms for T; maximal CaT requires between 25-50 ms while T requires 100 ms. In addition, time to peak T decreases with pulses shorter than 100 ms. Thus T amplitude is not determined solely by peak CaT.

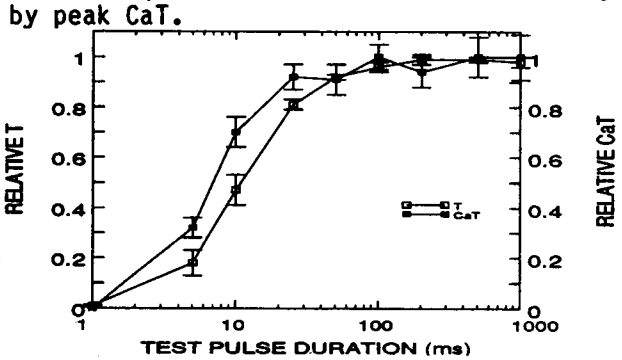

M-Pos557

EXTRACELLULAR Na DEPENDENT & INDEPENDENT DECAY OF THE $[Ca]_i$ TRANSIENT IN RAT CARDIAC MYOCYTES. J.R. Berlin#, D.M. Bers* and W.J. Lederer. #Bockus Research Inst., Philadelphia PA; *Un. of California at Riverside, Riverside CA; Un. of Maryland Sch. of Med., Baltimore MD.

The role of Na/Ca exchange and the sarcoplasmic reticulum (SR) in the decaying phase of the $[Ca]_i$ transient was examined in single rat ventricular cardiac cells. Cells were voltage-clamped with patch electrodes which contained 0.5 mM Na^+ and 70 μM indo-1. To determine the contribution of Na/Ca exchange, $[Ca]_i$ transients were elicited by depolarizing clamp pulses in 145 mM and 0 mM Na_o solutions (0Na). The declining phase of the transients were fitted as monoexponential functions. In 0Na, the decay rate constant (Tau) of the $[Ca]_i$ transient at the holding potential (V_h=-50 mV) was slowed 20±4% (n=5). At +15 mV, 0Na had a smaller effect on the rate of decrease of $[Ca]_i$. This indicates that Na/Ca exchange may contribute more significantly to relaxation at negative potentials than at plateau potentials. The Na_o-independent rate of decay of the $[Ca]_i$ transient was examined after repolarization to V_h. With 50 msec pulses in 0Na, larger $[Ca]_i$ transients were associated with faster decays of $[Ca]_i$ (Tau increasing 2-3 fold when peak $[Ca]_i$ increased from 0.3 to 1.5 μM). Following prolonged elevation of $[Ca]_i$ with 1 sec depolarizations, Tau was not as strongly influenced by the level of peak $[Ca]_i$. The mechanism responsible for the Na_o-independent decrease in $[Ca]_i$ (i.e. the SR) is rapidly influenced by the $[Ca]_i$ during the transient.

M-Pos558

CITRATE INHIBITS CARDIAC CONTRACTION BY AN EFFECT ON Ca CURRENT AND NOT BY SIMPLE Ca_o BUFFERING. Donald M. Bers, Larry V. Hryshko and Simon M. Harrison. Div. Biomed. Sci. Univ. of California, Riverside CA 92521.

Shimoni & Ginsberg (*Am J Physiol 252*:C248) showed that citrate (Cit) inhibited cardiac contractions and suggested that this was due to its Ca-buffering action (i.e. dissipating a local elevation of [Ca] at the outer sarcolemmal surface & thereby decreasing Ca influx). However, buffering Ca_o can limit Ca_o depletions (*Am J Physiol 256*:C813) and could thus allow *more* Ca entry. We compared the effects of 4 low affinity Ca buffers (Cit, NTA, DPA and ADA) on several cardiac preparations. In Mg-free medium with 2 mM free Ca (measured using murexide), Cit, DPA and ADA (10 mM) decreased twitch contraction in rabbit ventricle (to 75±2%, 60±3% & 86±2% respectively), but 10 mM NTA increased force slightly (to 106 ± 2%). There was no simple correlation between Ca affinity and the effect on tension. Nor were these effects due to changes in SR loading, since rapid cooling contractures were not affected and similar results were observed in the presence of caffeine or ryanodine. The depressant effects of Cit and ADA were greater at pH 5.5-6 and ADA had no effect at pH 8.5. Thus, the depressant effect is stronger with more protonated forms of the Cit & ADA, which are also poorer Ca buffers. Cit (& not NTA) greatly decreased Ca current (I_{Ca}) in whole cell voltage clamp. Thus, Cit (& some other bufers) may directly inhibit I_{Ca} independent of Ca buffering ability.

M-Pos559

REDUCED INTRAMEMBRANE CHARGE MOVEMENT IN DYSGENIC SKELETAL MUSCLE MYOTUBES. Kurt Beam and Brett Adams, Department of Physiology, Colorado State University, Fort Collins, CO, 80523.

Whole cell patch clamp was used to measure charge movement in myotubes from normal mice and mice with muscular dysgenesis. A prepulse protocol was used to immobilize Na channel and transient Ca channel gating charge. The pipette contained either Cs or TEA as the main internal cation. Internal TEA strongly inhibited calcium current but did not reduce charge movement. The saturating charge moved in dysgenic myotubes (2.3 nC/uF) was substantially less than that moved in normal myotubes (6.5 nC/uF). Because the dihydropyridine receptor, which is hypothesized to be the voltage sensor for E-C coupling, is mutated in dysgenic mice, the extra charge in normal myotubes probably represents movement of the voltage sensor that is missing in dysgenic myotubes. The origin of the residual charge in dysgenic myotubes is unclear, but may reflect gating of K channels.

Supported by grants from MDA (to KB) and from NIH (NS-24444 to KB and NS-08567 to BA).

M-Pos560

PROLONGED ELECTRICAL CONTROL OF MEMBRANE POTENTIAL (E_m) DURING TRANSPORT MEASUREMENTS BY INTERNAL DIALYSIS IN BARNACLE MUSCLE FIBERS. L.W. Horn, C.M. Philips. Dept. Physiol., Temple Univ., Phila. PA 19140

A voltage clamp with very low drift and high 60 Hz rejection has been designed for application of DC holding currents for hrs and determination of complete I-V curves or slope conductance (G). G is measured with a ¼ Hz, 2 mV p-p signal. Clamp records show classical behavior. The capacity transient is 95% complete in ~20 ms. Upon depolarization there is an early inward current which disappears in 0-Ca sea water, and an outward current which is inhibited by internal tetraethylammonium. G agrees well with I-V slopes in the -100 to -20 mV range. G, at holding potentials of -36 to -76 mV, is stable for 12 hrs of continuous dialysis and clamping with holding currents of 10 to 20 $\mu A/cm^2$, while the (100 ms) I-V curve shows only a small positive shift. Influx of L-glutamate, measured in the same experiment, is also stable. Depolarization produces a reversible decrease of glutamate influx, showing unequivocally that the transport is E_m-dependent. (Supported by NIH Grant NS18868).

M-Pos561

ADENYLIC CARRIER: KINETIC COMPLEXITY. F.E. Sluse, A. Evens, C. Duyckaerts and C.M. Sluse-Goffart, Lab of Bioenergetics, Univ. Liége, Belgium (Introduced by D. Zorov).

The kinetic approach of the adenylic carrier is very difficult because it seems that there is no proper time corresponding to the initial steady state. The time course of the electroneutral ADP/ADP followed to equilibrium in fast and semi-fast kinetic experiments shows an astonishing complexity: a 10 ms lag followed by a burst (sometimes structured) lasting about 150 ms then by a quasi-linear phase (till 1 or 2 s) and lastly by a rate decreasing phase till equilibrium.

Preincubation of mitochondria was carried out in the presence of cold ADP at a concentration such as the total ADP concentration is not changed when the exchange reaction is initiated by the addition of labelled ADP. It causes not only the quasi-disappearance of the complex fast phase but also the disappearance of one of the 3 exponentials needed to fit the time course from 0.3 to 1 s. Both could then be due to Frieden's type isomerization. It appears from these results that the adenylic translocator may exist under several interconvertible iso-forms and that different pools of internal ADP may be involved.

M-Pos562

DISCRIMINATION OF TWO DIFFERENT MECHANISMS FOR MITOCHONDRIAL Ca EFFLUX. E. Chávez, C. Zazueta and J.A. Holguín, Dept. Bioquímica, Inst. Nal. Cardiol ICH. México, D.F. 014080, Mexico (Introduced by M. Campo).

Mitochondrial Ca is released by several mechanisms. One of them is believed to be through an unspecific pathway which becomes operative by the oxidation of membrane -SH groups. Characterization of two different pathways for Ca release was made possible by using Hg at two concentrations. At high levels of Hg, Ca efflux is insensitive to the temperature of incubation, and the efflux rate is related to the internal free Ca concentration. At these levels of Hg bound, Sr is liberated similarly to Ca. At lower levels of Hg bound, Ca release is dependent on the incubation temperature and on the internal free Ca concentration. Under these conditions, Sr is not released. The results appear to indicate that depending on the level of Hg bound to the membrane, two different pathways for Ca release can be distinguished.

M-Pos563

MOLECULAR DETAILS OF THE E.COLI MANNITOL CARRIER ELUCIDATED BY DOMAIN SEPARATION AND COMPLEMENTATION

G.T. Robillard, R. van Weeghel, H. Pas, G. Meijer and W. Keck, Department of Chemistry, University of Groningen, Groningen, The Netherlands.

EII-mtl is a single 67 Kda polypeptide with a membrane-bound N-terminal half. The cytoplasmic portion possesses 2 phosphorylation sites, His 554 and Cys 384 which are essential for mannitol transport and phosphorylation. The C-terminal 145 residues shows homology with a water soluble EIII-mtl from S.aureus. Restriction sites were inserted at two positions in the gene which enabled us to subclone the entire C-terminal half, residues 348-637, the EIII-like domain, residues 490-637 and the N-terminal half, residues 1-347. The two C-terminal fragments were expressed as stable soluble cytoplasmic proteins which retained their in vitro mannitol phosphorylation activity when complemented with an EII-mtl inactive by virtue of a site-directed mutation of his 554 to ala. Both proteins have been purified. The N-terminal fragment was expressed as a stable membrane bound protein. Simultaneous transformation with plasmids expressing residues 1-347 and 348-637 resulted in cells which were able to grow on, and ferment mannitol. These experiments demonstrate that the E.coli mannitol carrier consists of three structurally and functionally distinct domains involving approximately residues 1-347, 348-489, and 490-637.

M-Pos564

AFFINITY-PURIFIED K^+ TRANSPORT PROTEIN FROM RAT LIVER MITOCHONDRIA. R. Paliwal, R. Bawa, and J. J. Diwan, Biology Department, Rensselaer Polytechnic Institute, Troy, NY 12180.

A protein fraction has been obtained from Triton-solubilized rat liver mitochondrial membranes by affinity chromatography on immobilized quinine, a K^+ transport inhibitor. The predominant protein in this fraction is estimated by SDS PAGE to be 53 kDa. Analysis via isoelectric focusing suggests that the affinity column eluate contains multiple polypeptides in the 53 kDa range. Immunoblots have shown the 53 kDa protein to be unrelated to F_1 ATPase subunits of similar size (Diwan, Haley, Kaftan, Joshi & Sanadi, Fifth EBEC Reports, 207, 1988). The column eluate has been reconstituted into phospholipid vesicles by detergent dialysis. Incorporation of the protein into the vesicles has been confirmed by SDS PAGE. Electrode recordings indicate that membranes reconstituted with the protein are leaky to K^+, but not to H^+ (Diwan, Haley, & Sanadi, BBRC 153: 224, 1988). When vesicles are pre-loaded with the fluorescent probe ANTS, the quenching of fluorescence by externally added Tl^+, a K^+ analog, is more rapid for vesicles incorporating the affinity-purified protein. Results obtained so far suggest that the quinine affinity column eluate may contain the mitochondrial K^+ uniporter. (Supported by USPHS Grant GM-20726).

M-Pos565

INHIBITION OF THE MITOCHONDRIAL INNER MEMBRANE ANION CHANNEL (IMAC) BY NUCLEOTIDE ANALOGS. Mary F. Powers and Andrew D. Beavis, Dept. of Pharmacology, Medical College of Ohio, Toledo, OH 43699.

IMAC transports a variety of anions and is inhibited by matrix Mg^{2+} and matrix H^+. Recently, Selwyn's group reported that agaric acid, Cibacron Blue, and palmitoyl CoA, which are inhibitors of the adenine nucleotide translocase inhibit IMAC at alkaline pH (EBEC Reports 5,205-206 (1988)). We have investigated these inhibitors in Mg^{2+}-depleted mitochondria and find that the extent of inhibition is dependent on the anion transported. Transport of Cl^-, NO_3^- and HCO_3^- is only partially inhibited (<60%), whereas transport of malonate is fully inhibited. This is reminiscent of the inhibition induced by mercurials. Other nucleotide analogs also inhibit IMAC in a similar manner: alizarin red S (IC_{50} 63.4 μM), bromcresol green (IC_{50} 10.6 μM), erythrosin B (IC_{50} 2.8 μM), rose bengal (IC_{50} 0.6 μM). Unlike inhibition by cationic amphiphiles, inhibition by these agents is not pH dependent indicating that these agents probably interact at a different site. This research was supported by NIH Grant HL 36573.

M-Pos566

A THIOL GROUP MAY MODULATE THE REGULATION OF THE MITOCHONDRIAL INNER MEMBRANE ANION CHANNEL (IMAC). Andrew D. Beavis, Dept. of Pharmacology, Medical College of Ohio, Toledo, OH 43699.

Treatment of mitochondria with N-ethyl-maleimide (NEM) modulates the inhibition of IMAC by matrix Mg^{2+}, matrix H^+ and propranolol. At pH 7.4 the pIC_{50} for H^+ is decreased from 7.8 to 7.4, the IC_{50} for Mg^{2+} is increased from 37 μM to 86 μM and the IC_{50} for propranolol is increased from 20 μM to 69 μM. As in the control mitochondria, these IC_{50} values are dependent on the pH of the assay medium suggesting that NEM does not react at the site which confers pH dependence. NEM has no effect on the Jmax (J extrapolated to $[H^+]=0$) of transport and this transport can be inhibited by mersalyl and p-Cl-mercuribenzenesulfonate (p-CMS). Thus, NEM does not appear to bind to the previously described mercurial-reactive inhibitory site. On the other hand, when transport is assayed in the presence of cysteine, it is evident that pretreatment with mersalyl and p-CMS leads to the same changes as pretreatment with NEM. Thus, all these sulfhydryl reagents appear to react at the same modulatory site. (This research was supported by NIH Grant HL36573).

M-Pos567

THE UNCOUPLING PROTEIN INDUCES ION CHANNELS IN PLANAR LIPID MEMBRANES. T.A.Mirzabekov, L.A.Pronevich, R.N. Achmerov* (Intro. by H.Tedeschi) Institute of Biological Physics Acad. Sci. USSR, Pushchino, USSR, 142292; *Institute of Physiology Acad. Sci. Uzbec SSR, Tashkent

The uncoupling protein from brown adipose tissue mitochondria of rats, newborn guinea-pigs and hibernating gophers (Citellus parryi) was isolated after Lin and Klingenberg (Biochemistry 21:2950;1982) and inserted into azolectin bilayers. One-sided addition of 1-5 ng/ml of the protein results in a discrete channels formation. Channel conductance equals 3.5; 3.2 and 4.0 nS in 1M KCl for protein from rats, newborn guinea-pigs and gophers, respectively. Conductance, voltage-dependence and selectivity of uncoupling protein channels were very similar to those reported for VDAC (mitochondrial porin channels). We suppose that the uncoupling protein isolated as in Ref. is always contaminated by mitochondrial porin. It is also possible that the uncoupling protein is the porin from brown adipose tissue mitochondria.

M-Pos568

MITOCHONDRIAL PHOSPHATE TRANSPORTER: AMINO ACID SEQUENCE AND EXPRESSION OF A FUSION PROTEIN IN E. COLI, G. C. Ferreira and P. L. Pedersen, Johns Hopkins University School of Medicine, Baltimore, MD.

A full-length cDNA clone encoding the rat liver mitochondrial phosphate transporter (H^+/P_i symporter) was isolated from a λgt11 library and sequenced. The mature protein comprises 312 amino acids and has a presequence of 44 amino acids. In order to express the mammalian transporter in bacterial cells, the P_i transporter gene was subcloned into the alkaline phosphatase promoter system, known to overexpress soluble proteins (e.g., mitochondrial ATP synthase α and β subunits), as well as fused to the ATP synthase α-subunit gene. The fusion protein, involving the α-subunit followed by the P_i transporter, was not detected by immunoblotting. However, directed-progressive deletions from the 3'end of the hybrid construct yielded a ladder of proteins (40 to 63 KDa), as detected by immunoblotting with polyclonal antibodies against the F_1 ATP synthase subunit. The deletion constructs were verified by DNA sequencing and the longest one corresponded to a fusion protein lacking the P_i transporter 60 COOH terminal amino acids. (Supported by NSF Grant DMB 8606759. GCF is a DR-WW Fellow, DRG 986).

M-Pos570

ATP INCREASES Na/Ca AND Na/Mn EXCHANGE IN RESEALED FERRET RED BLOOD CELL GHOSTS. M.D. FRAME and M.A. MILANICK. Dept. of Physiology,U. of Missouri, Columbia, MO 65212

Ferret red cells have high intracellular Na (140 mM). Na/Ca exchange activity (Ca influx) can be measured when the Ca pump is blocked by vanadate (AJP 256:C390). We prepared ferret red cell ghosts by hypotonic lysis. The restoring media included 5 mM ATP and hexokinase. After 15 min at 37°C, 10 mM glucose was added to half of the ghosts (low ATP). At 30 min. 1 mM vanadate was added (+V). The flux media contained (mM) 150 choline Cl, 20 HEPES (pH 7.4, 37 C), 0.05 DIDS, 0.05 Ca or Mn. ^{45}Ca influx was 6 fold greater in high ATP ghosts. ^{54}Mn influx was 5 fold greater in high ATP ghosts. In several other experiments Ca or Mn influx was increased 2 to 6 fold in high ATP ghosts. Mn influx was 1.6 fold higher in V-treated ghosts.

[ATP]	FLUX*		
mmol/lpg	Ca (+ V)	Mn (+ V)	Mn (-V)
low < 0.1	0.42	0.44	0.27
high >3.0	2.56	2.15	1.32
*units: mmol/(l packed ghost/h) (s.e. < 10 %)			

One mechanism that explains the effects of ATP and vanadate is that Na/Ca exchange is increased in the phosphorylated state, where ATP is a Pi donor and vanadate inhibits phosphatase activity.(NIH DK-37512, AHA MO Aff.)

M-Pos569

PURIFICATION AND CHARACTERIZATION OF THE RECONSTITUTIVELY ACTIVE TRICARBOXYLATE TRANSPORTER FROM RAT LIVER MITOCHONDRIA. R.S. Kaplan, J.A. Mayor, N. Johnston, and D.L. Oliveira. Univ. of South Alabama, Coll. of Medicine, Mobile, AL 36688.

Procedures have been developed for the preparation of highly purified, active tricarboxylate transporter from rat liver mitochondria. The transporter is extracted from mitoplasts with Triton X-114 and is then sequentially chromatographed on hydroxylapatite, Matrex Gels Orange A and Blue B, and Affi-Gel 501. Upon incorporation into phospholipid vesicles, the final mercaptoethanol-activated Affi-Gel 501 eluate catalyzes a 1,2,3-benzenetricarboxylate-sensitive citrate/citrate exchange with a specific activity of 3240 nmol/4 min/mg protein. This value is enhanced 831-fold with respect to the initial detergent extract. Analysis via SDS-PAGE indicates the presence of one major protein band with a molecular mass of approx. 32.5 kDa. We have characterized the substrate specificity and the inhibitor sensitivity of the reconstituted purified transporter. Most interestingly, the transporter is inhibited by reagents that are relatively selective for sulfhydryl, histidyl, guanidyl, and lysyl residues. (Supported by NIH grant 5R29GM-38785 to R.S.K.).

M-Pos571

A COMPARISON OF THE PROPERTIES OF THE Na/Ca EXCHANGER FROM SARCOLEMMA AND ROD OUTER SEGMENTS **Barrios, B., Nicoll, D.A., and Philipson, K.D.; Cardiovascular Research Laboratory, UCLA School of Medicine, Los Angeles, CA 90024-1760.**

The properties of the Na/Ca exchangers from cardiac sarcolemma (SL) and rod outer segments (ROS) were studied in parallel by measuring the Na-gradient dependent Ca-uptake into SL or ROS vesicles. The ROS exchanger, but not the SL exchanger, was stimulated by K^+ with an apparent K_M of 0.2 mM. The addition of valinomycin, to produce an inside-positive membrane potential, stimulated the SL exchanger 1.8-fold and the ROS exchanger 1.2-fold. The K_M's and V_{max}'s for Ca for the exchangers were estimated to be 20 uM and 8 nmol mg^{-1} s^{-1} in SL and 5 uM and 1 nmol mg^{-1} s^{-1} in ROS. Both exchangers were stimulated by proteases and phospholipase D. Unlike the SL exchanger, however, the ROS exchanger was neither stimulated by intravesicular Ca nor inhibited by intravesicular EGTA.

M-Pos572

ON THE NATURE OF ION LEAKS IN THE MITOCHONDRIA INNER MEMBRANE. Xiaocheng Sun, Weihua Li and Keith D. Garlid, Department of Pharmacology, Medical College of Ohio, Toledo, Ohio 43699.

The validity of a model by Garlid et al. (BBA, in press) to describe the nature of ion leaks was tested by measuring $\Delta\Psi$-dependent fluxes of $H^+(H_3O^+)$ and TEA^+. J_{x+} is non-ohmic over the range 130-200 mV, as previously observed. Moreover, as predicted by the model, ln(J) is linear with $zF\Delta\psi/RT$ with slope = 0.5, indicating a barrier peak located at the center of the insulating membrane. Apparent permeability coefficient for H_3O^+ is 10^6 - 10^7 times greater than P for TEA^+ or Li^+. If this were due to differences in conductance mechanism across the bilayer, Ea for H^+ should be 40-50 kJ lower than that for TEA^+, but is only 25 kJ lower, and some of this difference can be attributed to TEA^+ dehydration. Li^+, Mg^{2+}, quinine and H^+ itself each inhibit TEA^+ conductance but have no effect on H^+ conductance. These data suggest that H_3O^+ and hard cations cross the barrier by fundamentally similar mechanisms and that differences in apparent P reside at the interface. Supported by NIH Grant GM 31068.

M-Pos573

COMPETATIVE INTERACTION BETWEEN Rh123, Ca^{+2}, H^+, AND CCCP BINDING TO MITOCHONDRIA. J.R. Bunting, *Baylor Research Foundation, Dallas, Tx., 75226.* Mitochondria are important sinks for cellular cations. Factors affecting their selective sequestration and relationship with the trans membrane potential (TMP) are not well understood. Studied here is the effect of variation of external concentration of cations important to rat liver mitochondrial (RLM) function on the TMP as probed using fluorescent potential probe Rh123. Alteration in TMP was recorded during variation of proton, calcium ion, and lipophilic protonophore, CCCP. Increased addition of these ions to respiring RLM resulted in reduction of the apparant TMP with relative 50% potency of 68 nM, 2.2 μM, and 72 μM for CCCP, H^+ and Ca^{+2}, respectively. Lineweaver-Burk plots of inhibition of binding of increasing amounts of Rh123 to RLM in the presence of various inhibitory concentrations of Ca and CCCP demonstrate competative inhibition between the ions and their site of interaction with the TMP. This suggests a common site of interaction of these agents with the apparatus establishing the apparant RLM membrane potential.

M-Pos574

PROGRESS TOWARD MOLECULAR CHARACTERIZATION OF THE K^+/H^+ (Na^+/H^+) ANTIPORTER FROM RAT LIVER MITOCHONDRIA. Xianqiang Li, Department of Pharmacology, Medical College of Ohio, Toledo, Ohio 43699.

The SDS-denatured, 82 kDa K^+/H^+ antiporter from rat liver mitochondria was purified and used to raise and immunopurify polyclonal antibodies, which proved to be monospecific. I now report on purification of the native antiporter protein, using both [^{14}C]DCCD-labeling and Western blot analysis to follow purification. Mitochondrial proteins were extracted with Triton buffer, fractionated with $(NH_4)SO_4$, and separated on DEAE-Sephadex, Phosphocellulose and Hydroxylapatite. These steps resulted in approximately 100 μg of antiporter from 500 mg mitochondrial proteins. Reconstitution of the purified antiporter preparation into proteolipid vesicles resulted in electroneutral $^{86}Rb^+$ and K+ transport that was inhibited by DCCD and quinine. The N-terminal sequence of the purified 82 kDa antiporter protein was determined and does not show homology with any published protein sequence. This research was supported in part by NIH Grant HL 36573.

M-Pos575

A KINETIC MODEL FOR THE E.COLI MANNITOL TRANSPORT PROTEIN

J.S. Lolkema and G.T. Robillard
Physical Chemistry Department
State University of Groningen
The Netherlands

The mannitol transporter of E.coli, EIImtl, is part of the P-enol-pyruvate dependent phosphotransferase system: transport accros the cytoplasmic membrane is coupled to phosphorylation of the sugar. A kinetic model is presented based upon the kinetics of mannitol phosphorylation catalyzed by EIImtl embedded in the native membrane of closed or open vesicular structures or solubilized in detergent. This approach allows us to discriminate between kinetic pathways of phosphorylation that are or are not coupled to transport steps. In addition the effects of detergent on the kinetic behaviour can be analyzed.

M-Pos576

A RAPID METHOD FOR RECONSTITUTION OF BACTERIAL MEMBRANE PROTEINS. Atul Varadhachary and Peter Maloney, Dept of Physiology, The Johns Hopkins University School of Medicine, Baltimore, MD-21205.

We present a technique for solubilisation and reconstitution of bacterial membrane proteins directly from small (1-20 ml) volumes of cell culture, eliminating preparation of membrane vesicles. Cells are subjected to simultaneous lysozyme digestion and osmotic lysis, then pelleted. The ghosts are solubilised in 1.2% β-octyl D-glucopyranoside (w/v) in the presence of added lipid and an osmolyte. After clarification by centrifugation, aliquots were used for reconstitution. Controls exclude contribution by contaminating whole cells or membrane vesicles. Transport characteristics of proteoliposomes prepared using this rapid approach are similar to those using standard methods. Proteoliposomes are non-leaky, and a membrane potential can be generated and sustained. We have used this approach to reconstitute three membrane carriers solubilised from three different gram-negative species. Functional porins do not reconstitute. We feel that this method will be of importance when screening and characterising a large number of strains, both wild type and mutant.

M-Pos577

UHPT - THE SUGAR PHOSPHATE TRANSPORTER OF *ESCHERICHIA COLI* IS FUNCTIONAL AS A MONOMER. S.V. Ambudkar*, V. Anantharam and P.C. Maloney. Departments of Physiology and *Medicine, The Johns Hopkins University School of Medicine, Baltimore, MD. 21205.

UhpT, the product of the *uhpT* gene of *E. coli*, is a 51-kDa membrane protein that catalyzes glucose 6-phosphate : phosphate (G6P : Pi) antiport. We have used a reconstitution assay to determine whether monomeric or oligomeric structures are required for function. The following observations suggest that the monomeric form is fully functional. (1) During HPLC gel filtration of the detergent extract, transport activity migrates in the 50 to 56-kDa range. (2) For these same conditions, treatment of solubilized UhpT with pyridoxal 5'-phosphate and $NaBH_4$, results in irreversible inactivation of antiport; among sugar phosphates tested only substrates (G6P, 2DG6P) protect the transporter from such inhibition. (3) The initial rate of G6P transport by proteoliposomes varies linearly with increasing protein to phospholipid ratios in a range (1:500 to 1:5,000), where it is expected that there is less than one functional unit per proteoliposome.

M-Pos578

THE SODIUM/IODIDE SYMPORTER: EXPRESSION IN OOCYTES AND STUDIES WITH INHIBITORS Franck Vilijn, Kari Koszdin, Stephen Kaminsky and Nancy Carrasco Department of Molecular Pharmacology, Albert Einstein College of Medicine, Bronx, NY, 10461 USA.

The iodide carrier of the thyroid gland is a membrane protein responsible for the active, Na^+-dependent accumulation of iodide by the thyroid follicular cells, a process induced by TSH via cAMP. Iodide uptake is the first step in the synthesis of thyroid hormones T3 and T4. We report the expression of iodide transport activity in *Xenopus laevis* oocytes microinjected with mRNA isolated from FRTL-5 cells, a line of highly differentiated rat thyroid cells whose growth and iodide uptake activity are markedly dependent on TSH. A 7-fold increase of Na^+-dependent, ClO_4^- sensitive iodide transport activity (an average of 3.5 pmoles of [125]iodide per oocyte in 45 min) is observed in oocytes microinjected with mRNA from FRTL-5 cells maintained in the presence of TSH over control oocytes (~0.5 pmoles), including those microinjected with mRNA from FRTL-5 cells maintained in the absence of TSH. Sucrose gradient fractionation of mRNA followed by injection of fractions revealed that the mRNA encoding the transporter is 2.4 to 4.0 kb in length.

Iodide transport in plasma membrane vesicles is shown to be inhibited by harmaline-like compounds and kinetic studies indicate they compete with sodium.

M-Pos579

CONDITIONS FOR A NEGATIVE SLOPE IN THE CURRENT-VOLTAGE RELATIONSHIP OF THE Na/K PUMP IN *XENOPUS* OOCYTES. R.F. Rakowski, L.A. Vasilets and W. Schwarz. Max-Planck-Institut für Biophysik, Frankfurt/M, F.R.G.

Experimental conditions required to produce a negative slope in the current-voltage relationship (I-V) of the Na/K pump in Xenopus oocytes have been examined. Defolliculated oocytes were Na-loaded by Ca^{2+} and K^+-free incubation. Experimental solutions contained (in mM) 5 $BaCl_2$, 20 tetraethylammonium Cl (to block passive K conductance), 2 $CaCl_2$, 5 TRIS/MOPS buffer (pH = 7.6), various KCl, and either 90 NaCl or 90 tetramethylammonium Cl. Changes in steady-state I-Vs produced by 50 μM ouabain or K-free solution were measured. Repeated I-V measurements demonstrated the absence of drift with time. In Na-free solution the Na/K pump I-V in 5 mM K was nearly voltage-independent, but reducing external [K] to 0.1 or 0.25 mM produced a negative slope over the range -100 to 0 mV. The Na/K pump I-Vs obtained in 90 mM Na and 5 mM K were monotonic saturating sigmoid functions of voltage, while I-Vs in 1 or 2 mM K had a negative slope above 0 mV. These findings suggest the existence of more than one voltage-dependent step in the Na/K pump cycle. Supported by DFG and by NIH.

M-Pos580

REGULATION OF THE Na,K,Cl-COTRANSPORTER IN TUBULES ISOLATED FROM SHARK RECTAL GLAND. Chris Lytle, Stephanie Lear and Bliss Forbush III, with the assistance of Mark Weinberg and Christina Forbush. Mt. Desert Is. Bio. Lab., Salsbury Cove, ME, 04672, Dept. of Physiol. Yale Univ. School of Medicine, New Haven, CT, 06510, and Renal Unit, Beth Israel Hospital, Boston MA 02215.

The Na,K,Cl-cotransporter in dogfish shark rectal gland is up-regulated as part of the overall process of hormonal stimulation of fluid secretion (Forbush and Haas, Biophys. J. 55, 422a, 1989). We have studied this process in further detail by examining [^{3}H]benzmetanide (Bz) binding to collagenase-isolated tubules from the rectal gland. In a typical experiment, isolated tubules were incubated in pre-oxygenated HEPES-buffered shark Ringers solution with 0.5 µM Bz for 30 min at 20°C; the amount of Bz bound to membranes was determined after Millipore filtration. We found that specific Bz binding was dramatically increased (from ~1-5 pmol/mg protein to ~30 pmol/mg protein) when the tubules were stimulated by forskolin, VIP, or 8-CPT cAMP, agents known to produce maximal stimulation of secretion. The activation by forskolin, measured at 1 min intervals in a rapid binding assay, was half maximal in 3 min. Activation of O_2 consumption, measured in parallel, followed the same time course. Cell shrinkage was equally effective in stimulating binding. A 70% increase in tonicity by sucrose addition produced maximal stimulation ($t_{1/2}$ = 3 min) and a 40% increase in tonicity had a half-maximal effect. Stimulation of binding was rapidly reversed on resuspension of shrunken tubules in isotonic medium (910 mOsm; $t_{1/2}$ ~2.5 min). Paradoxically, Bz binding was also stimulated by cell swelling, with 45% activation at 700 mOsm. Both shrinkage-induced and swelling-induced Bz binding required extracellular Na and Cl. These findings support a model in which up-regulation of Na,K,Cl-cotransport is an important step in the hormonal stimulation of secretion, and they suggest that cell volume could play a role in the control process. (Supported by AHA CT-201-889 and NIH AM17433).

M-Pos582

PROLYL RESIDUES ARE NOT ESSENTIAL FOR THE MECHANISM OF LACTOSE TRANSPORT IN THE *LAC* PERMEASE OF *E. COLI*. THOMAS G. CONSLER, ORESTES TSOLAS, AND H. RONALD KABACK, DEPT. PHYSIOL., & MBI, HHMI/UCLA, LOS ANGELES, CA 90024-1570, USA.

The *lac* permease of *E. coli* is a hydrophobic plasma membrane protein that catalyzes the coupled translocation of a single β-galactoside with a single H^+. The permease has been solubilized from the membrane, purified to homogeneity and demonstrated to be solely responsible in the form of a monomer for β-galactoside transport. Each of the 12 prolyl residues in *lac* permease has been systematically replaced with gly, ala and leu or deleted by truncation of the c-terminus. At least one of these replacements at each position resulted in a mutant permease that retained significant active transport activity. The concentration of each of the mutant permeases in the membrane is comparable to that of wild-type permease as judged by immunological analyses. The results indicate that it is primarily a chemical property of the side chain at the positions described (i.e., bulk, hydropathy and/or ability to hydrogen bond) that is critical for *lac* permease activity and that neither cis/trans isomerization of prolyl residues nor the presence of kinks at these positions is important.

M-Pos581

KINETICS OF PROTON TRANSLOCATION ACROSS AND ALONG MEMBRANES AS MONITORED BY OPTICAL pH-INDICATORS LOCATED AT THE SURFACE OF BACTERIORHODOPSIN OR OF THE LIPID BILAYER **J. Heberle and N.A. Dencher**
Dept. Physics/Biophysics, Freie Universität, Arnimallee 14, D-1000 Berlin 33, FRG.

Time-resolved spectroscopy of optical pH-indicators was employed to: 1. determine surface pH and potential of the purple membrane (PM), 2. correlate H^+ release and reuptake by bacteriorhodopsin (BR) with the formation and decay of photocycle intermediates, and 3. judge the recent proposal that protons move faster along the membrane surface than in the aqueous bulk phase. Signals of the pH-indicator pyranine in the bulk phase were compared with those of fluorescein covalently linked to BR or to the lipid head group of DPPE. From the data obtained with labelled BR residing in PM or in reconstituted vesicles as well as with BR/DMPC vesicles doped with F-DPPE it can be concluded that the kinetics of H^+-translocation across BR can only be accurately determined with an indicator bound to BR. The H^+ released by BR with e.g. a time constant of 5 µs is monitored by pyranine in the aqueous bulk phase with τ=190 µs. We have no indication for faster H^+-movement along the membrane surface.

M-Pos583

OSMOTIC STIMULATION OF Na^+, K^+, Cl^- COTRANSPORT IN SQUID GIANT AXON IS $[Cl^-]_i$-DEPENDENT. G.E. Breitwieser, Johns Hopkins Univ., Baltimore, MD, A.A. Altamirano and J.M. Russell, UTMB, Galveston, TX.

Bumetanide-sensitive (B-S) Cl^- influx (but not Cl^- efflux) into internally dialyzed squid giant axons was stimulated by hyperosmotic external fluid, but only when $[Cl^-]_i \geq 100$ mM. At $[Cl^-]_i$ = 150 mM, B-S Cl^- influx was directly related to extracellular osmolality (π_o) adjusted between the normal π_o = 975 mOsmol/kg up to π_o = 1170 mOsmol/kg by mannitol addition. At π_o = 975 mOsmol/kg, intracellular Cl^- inhibited the B-S Cl^- influx in a $[Cl^-]_i$-dependent fashion ($K_i \simeq 90$ mM). However, at π_o = 1170 mOsmol/kg the relationship between $[Cl^-]_i$ and B-S Cl^- influx shifted towards higher $[Cl^-]_i$ values ($K_i \simeq 125$ mM). Thus, treatment with hyperosmotic external fluid stimulated B-S Cl^- influx at physiological $[Cl^-]_i$ levels (120 mM) which, under normo-osmotic conditions, would almost completely inhibit the Na^+, K^+, Cl^- cotransporter.
Supported by NIH NS-11946 (JMR).

M-Pos584

MEASUREMENT OF SUGAR-INDUCED CURRENTS IN LLC-PK$_1$ EPITHELIAL CELLS USING WHOLE CELL RECORDING TECHNIQUES

E. Bennett, C. Smith-Maxwell, J. Randles, and G.A. Kimmich, Intro. by W. Bernhard, Dept. of Biophysics, U. Rochester, Rochester, NY 14642

Current-voltage relationships were determined for Na^+-coupled sugar transport in LLC-PK$_1$ cells using whole cell recording techniques. Alpha-methylglucoside (AMG)-induced currents were observed under conditions of either inwardly directed (Case A: 154 Na^+_o, 10 AMG_o; 0 Na^+_i, 0 AMG_i; in mM) or outwardly directed (Case B: 10 Na^+_o, 1 AMG_o; 180 Na^+_i, 10 AMG_i) Na^+ and sugar gradients. Sugar-induced negative currents at hyperpolarized potentials (eg., -20pA at -90mV) that reversed at +54mV were observed in Case A. The current returned to basal levels by addition of 320uM external phlorizin. Induced currents of the opposite polarity were seen under Case B conditions (+12pA at +30mV, reversing at -128mV). The sugar-induced current was detected through inhibition by 800uM external phlorizin. Recordings were taken from 33 cells. Polarities of the sugar-induced reversal potentials in all cells and the magnitude of the reversal potential in Case B are consistent with thermodynamic predictions describing a $2Na^+$:1sugar transport system. **- Supported by USPHS-DK15365-18**

M-Pos585

REVERSE PHOTOVOLTAGE ASSOCIATED IN M TO BR BACKPHOTOREACTION OF A DEHYDRATED ORIENTED PM FILM AND ITS TECHNOLOGICAL APPLICATION.

H. Takei†, A. Lewis*† and Z. Chen†. †Dept. of Applied Physics, Cornell U., Ithaca, NY 14853 and *Dept. of Applied Physics, The Hebrew U. of Jerusalem, Israel.

When an oriented PM film prepared by an electrophoretic method is treated with a high pH (10) buffer and subsequently dehydrated, the M intermediate is significantly stabilized. When such a film is exposed to blue light following yellow light illumination, the film exhibits a reverse photovoltage. The amplitude of the reverse photovoltage depends on the time delay between the yellow and blue light. When compared with the recovery rate of the bR state as observed spectrophotometrically, the decay rate of the reverse photovoltage amplitude is much slower. This may indicate that not all M components lead to the reverse photovoltage.

The reverse photovoltage offers technologically interesting possibilities. The PM film can be viewed as a light-to-electrical signal transducer whose output polarity can be controlled. Such a transducer capable of excitatory and inhibitory responses at the molecular level adds a new dimension to the field of optoelectronics. We present edge detection as one application that fully exploits this property.

M-Pos586

A ^{31}P NMR SATURATION TRANSFER STUDY OF THE ADENINE NUCLEOTIDE TRANSLOCASE.

P.T. Masiakos*, D. Berkich*, G.D. Williams^, M.B. Smith*^, and K.F. LaNoue*, *Dept. of Cellular & Molecular Physiology, ^Dept. of Radiology, Division of NMR Research.

^{31}P-NMR measurements of saturation transfer have been used to monitor the reaction catalyzed by the mitochondrial adenine nucleotide translocase and the kinetic controls of this process in intact, functional mitochondria.

Results from the application of this technique to respiring liver mitochondria indicate that at 8°C the flux is 890±37 (n=5) nmoles min^{-1} mg^{-1}, approximately ten times faster than previously reported values obtained isotopically. Differences are probably due to the fact that the previous biochemical measurements required the use of oligomycin to inhibit the ATPase. We have found that this inhibition lowers matrix ATP levels and adversely affects the translocase flux. Experiments are underway to determine the K_m of matrix ATP and the K_i of external ADP in both liver and heart mitochondria. Extrapolation of the results to ADP and ATP levels measured in intact tissues will permit prediction of the circumstances where ATP synthesis is rate limiting for respiratory metabolism.

M-Pos587

EXPRESSION OF ARTEMIA Na/Ca EXCHANGE ACTIVITY IN XENOPUS LAEVIS OOCYTES.

Joo Cheon and John P. Reeves, Roche Institute of Molecular Biology, Roche Research Center, Nutley NJ 07110 USA

Na/Ca exchange activity in membrane preparations from developing *Artemia* attains half-maximal levels at about the time of hatching (Arch. BB 267:736, 1988). Poly(A)RNA was prepared from hatching *Artemia* nauplii and injected into *Xenopus laevis* oocytes. Three days after injection, the oocytes were loaded with Na by treatment with 30 uM nystatin in the presence of 100 mM NaCl. Na/Ca exchange activity was measured as the difference in 45-Ca uptake (20 uM, 10 min at room temp.) in 100 mM KCl minus that in 100 mM NaCl. Water-injected control oocytes showed virtually no activity (0.17 pmol per oocyte) whereas activity was high (3.73 pmol per oocyte) with the poly(A)RNA-injected oocytes. In the absence of the nystatin treatment, no activity was observed in either batch of oocytes. After size-fractionation by sucrose density gradient centrifugation, activity was enriched in the fraction containing poly(A)RNA between 0.5 and 2.0 kb. SDS-PAGE of the in vitro translation products of this fraction revealed proteins of less than 70 kDa. These results suggest that the *Artemia* exchanger may be a relatively small mol.wt. protein (<70 kDa). Experiments are under way to obtain expression from a cDNA library prepared from size-fractionated *Artemia* poly(A)RNA.

M-Pos588

PARTIAL PURIFICATION AND IDENTIFICATION OF THE SODIUM/CALCIUM EXCHANGER FROM BOVINE CARDIAC SARCOLEMMA. John T. Durkin, Diane C. Ahrens, and John P. Reeves. Roche Institute of Molecular Biology, Nutley, NJ, 07110.
Sarcolemmal vesicles are alkaline extracted (Philipson *et al.*, 1987, BBA 899, 59), solubilized in 2% cholate in 30 mM NaCl, applied to heparin-agarose, and eluted with 500 mM NaCl. Specific activity increases 10-15 fold, and the eluted material is greatly enriched in a band at 150 kDa on SDS-PAGE. Both Na/Ca exchange activity and the 150 kDa protein bind to WGA-Sepharose in a detergent-dependent manner and elute with 0.1% polyoxyethylene-9-lauryl ether, as reported previously for exchange activity (Durkin *et al.*, 1988, Biophys.J. 53, 141a). When the material eluted from WGA-Sepharose is fractionated by Mono-Q anion exchange, the 150 kDa band parallels the distribution of activity and constitutes more than 80% of the protein in the active fractions. Other minor bands are present, but only one (at 130 kDa) parallels the distribution of activity. Specific activities near 1 μmol / (mg protein x s) have been observed. We tentatively identify the 150 kDa band as the Na/Ca exchange carrier.

M-Pos589

A SIMPLE METHOD FOR MONITORING MITOCHONDRIAL PH GRADIENTS IN INTACT CELLS. P.J. Thomas, L.G. Gaspers, C. M. Pharr, and J.A. Thomas, Dept. of Biochemistry and Molecular Biology, University of South Dakota School of Medicine, Vermillion.

Unlike most intracellular pH indicators such as BCECF, fluorescein freely distributes between the cytosolic and mitochondrial compartments. As is typical for weak acids, the distribution between these compartments is governed by the magnitude of the pH gradient. Since fluorescein has two ionizable groups, a pH gradient of 1 results in an 80-fold concentration increase in the mitochondrial compartment. In addition, the mitochondrial dye spectra are red-shifted by approximately 8 nm. This permits qualitative monitoring of mitochondrial pH transitions by dual wavelength spectroscopy ($A_{510} - A_{540}$). If the cytosolic pH is known, the mitochondrial pH can be quantitated, based on the extinction coefficients for the ionized indicator in the mitochondrial and cytosolic compartments and the percentage mitochondrial volume. With isolated mitochondria, this method gives results in agreement with those obtained from the distribution of radioactive 5,5-dimethyloxizolidine-2,4-dione (DMO).

Supported in part by a grant from The USD/Parsons Medical Research Fund.

M-Pos590

EXTRUSION KINETICS OF Ca^{2+} FROM HUMAN PLATELETS IN THE 0.5 TO 10μM CYTOPLASMIC Ca^{2+} RANGE. P.A. Valant, P.N. Adjei, J.S. Johansson, and D.H. Haynes. Dept. of Pharmacology, Univ. of Miami School of Medicine, Miami FL 33101

The kinetics of Ca^{2+} extrusion from Rhod-2 loaded platelets was monitored by a series of manipulations described recently by Johansson and Haynes, J. Membrane Biol. 104:147-163, 1988. The technique was applied to Rhod-2 to probe Ca^{2+} efflux in a higher range of cytoplasmic Ca^{2+} ($[Ca^{2+}]_{cyt}$). The Ca^{2+}-sensitive fluorescent probe, Rhod-2 was loaded to cytoplasmic levels of 2-3 mM (1.5 hrs, 23°, 12μM Rhod-2/AM). Cellular hydrolysis produced a high affinity form (Kd of 500 to 1000nM) and a low affinity form (Kd of 1.4 mM). These corresponded to 20% and 80% of intracellular dye, respectively. To monitor Ca^{2+} efflux $[Ca^{2+}]_{cyt}$ was raised to 10 μM by addition of ionomycin in the presence of external Ca^{2+}. Immediately after, EGTA was added to remove external Ca^{2+}. In the presence of Na^+, plots of rate (-dFl/dt) vs $[Ca^{2+}]_{cyt}$ (0.1-10 μM) showed saturation kinetics with an apparent Km of 0.5-1.0 μM Ca^{2+}. Removal of Na^+ by Na^+ replacement with $NMDG^+$, choline or K^+ slowed its Vmax to 45%, 17% or 13% of the original value, respectively. These results indicate that between 0.5-10 μM$[Ca^{2+}]_{cyt}$, the extrusion process is dominated by Na^+-Ca^{2+} exchange. Supported by FL/AHA and NIH HL 38228.

M-Pos591

CCCP EFFECTS ON THE NAK-ATPASE PROTEOLIPOSOMES. Atsunobu Yoda and Shizuko Yoda, Department of Pharmacology, University of Wisconsin Medical School, Madison, WI 53706

In the NaK-ATPase proteoliposomes (PLs), the NaK-pump activity was enhanced by a proton ionophore, CCCP. This activator is thought to be due to the enhancement of proton mobility (= an increase in conductance) across the lipid bilayer, resulting in a decrease of the membrane potential. Although our previous study indicated that CCCP enhanced the change of E_1P to E_2P, the question of which step in the $E_1P \rightarrow E^*P \rightarrow E_2P$ reaction is activated by CCCP remains unsolved. When PLs containing K^+ inside were phosphorylated at 15°C using 20 μM ATP and 20 μM palmitoyl CoA instead of a high ATP concentration, the presence of 1 μM CCCP increased E*P content from less than 5% to > 20% and decreased E_1P content from 95% to < 80%. These results suggest that the change of E_1P to E*P is activated by CCCP. Therefore, the CCCP activation step in the NaK-pump, i.e., the E_1P to E*P conversion, seems to also be the voltage-sensitive step. (Supported by NIH Grant HL16549)

M-Pos592

MEASUREMENT OF FREE Mg^{2+} IN ISOLATED HEART MITOCHONDRIA. B. A. Hogue and R. G. Hansford. Laboratory of Cardiovascular Science, NIA, Baltimore, MD.

We have loaded suspensions of rat heart mitochondria with the fluorescent probe Mg-fura-AM, in a protocol which preserves respiratory control ratios >5. Excitation at 345 and 370nm, using a PTI Deltascan, produces emission at 510nm which is 5x autofluorescence and which is Mg^{2+}-sensitive. The signal is calibrated by equilibration with extramitochondrial Mg^{2+} (Rmin with EDTA and Rmax with 45mM Mg^{2+}) using Br-A23187 (5μM), in the presence of nigericin (5μM) and rotenone (2μM). Autofluorescence of unloaded mitochondria is subtracted prior to determining the 345/370nm ratio. During oxidation of glutamate plus malate in a medium containing 0.12M KCl, 1mM Pi and 1mM Mg^{2+}, matrix free Mg^{2+} ($[Mg^{2+}]_m$) was found to be 0.82±0.02mM (n=4): raising the Mg^{2+} in the medium to 2mM did not raise $[Mg^{2+}]_m$ significantly. Inclusion of the polyamine spermine (2mM) markedly increased $[Mg^{2+}]_m$, with the 345/370nm ratio indistinguishable from Rmax. These findings are relevant to the control of pyruvate dehydrogenase interconversion by Mg^{2+} and polyamines.

M-Pos593

TWO PATHWAYS OF PASSIVE Ca^{++} MOVEMENT ACROSS THE HUMAN RBC MEMBRANE. S. A. Desai. Washington University, St. Louis, MO.

I examined the kinetics of transmembrane Ca^{++} movement in human RBCs pretreated with iodoacetamide and vanadate to inactivate the Ca^{++} extrusion pump. Unidirectional influx rates were adequately fitted by an equation consisting of a saturable component (V_{max} = 332 ± 18 nmol/gm dry wt * h and K_m = 1.35 ± 0.13 mM) and a nonsaturable component (P = 7.2 ± 0.6 * 10^{-11} cm/sec). The two terms in this equation represent independent, parallel pathways of passive Ca^{++} movement. The saturable component mediates efflux as well as influx, and exhibits bidirectional acceleration by unlabeled trans Ca^{++}. External Sr^{++} competitively inhibited Ca^{++} influx through the saturable pathway (K_i = 12.7 ± 1.4 mM) and accelerated Ca^{++} efflux. Ca^{++} transport through this pathway has a Q_{10} of 2.7. In contrast, the nonsaturable component is inhibited poorly by Sr^{++} (K_i = 90 ± 29 mM) and has a Q_{10} of 1.4, in good agreement with the prediction of the Stokes-Einstein equation. I conclude that the saturable pathway is a simple Ca^{++} carrier for which Sr^{++} is an alternate substrate, whereas the nonsaturable pathway is a pore for the aqueous diffusion of Ca^{++}.
(Supported by grants TG AI 07172, HL 12839, and 5T32 GMO 7200).

M-Pos594

INTRACELLULAR Cl^- DEPENDENCE OF HYPERTONICALLY ACTIVATED Na-H EXCHANGE ACTIVITY IN BARNACLE MUSCLE. Bruce A. Davis, Emilia M. Hogan and Walter F. Boron. Dept. Cell. & Molec. Physiol., Yale Univ. Sch. of Med., New Haven CT 06510

We had previously characterized the presence of an amiloride-sensitive Na-H exchange activity in barnacle muscle fibers (BMF). Parker et al. earlier had reported that stimulation of Na-H exchange by shrinkage of dog RBCs requires the presence of Cl^-. However, is was not determined if this chloride dependence was intra- or extracellular. We examined this question using internally dialyzed BMFs. The net H^+ flux was determined from the rate of pH_i change (dpH_i/dt) and buffering power (β). In BMFs exposed to artificial seawater (ASW) having an osmolality of 1600 mOsm/kg (hypertonic to the standard osmolality of 975), β was 63 mM/pH at pH_i 6.8. When SITS-treated BMFs were exposed to a hypertonic ASW containing 50 mM Na^+ ($[Cl^-]_i$=34 mM, $[Cl^-]_o$=554 mM), 1 mM amiloride reduced the H^+ flux by 0.30 mM/min. BMFs dialyzed with fluid containing 34 Cl^- and exposed to Cl^- free hypertonic ASW containing 50 mM Na^+ ($[Cl^-]_i$=34, $[Cl^-]_o$=0) also exhibit an amiloride-sensitive H^+ flux of 0.30 mM/min. However, when Cl^- is removed from both the inside and outside, the amiloride-sensitive H^+ flux is only 0.06 mM/min. These results indicate that the Na-H exchange activity activated by hypertonicity in the BMF requires the presence of intracellular Cl^-.

M-Pos595

EFFECT OF EXTERNAL Ca^{2+} (Ca_o) ON VOLUME RESPONSE TO HYPOTONIC STRESS IN BARNACLE MUSCLE CELLS. D. M. Berman., E. M. Santiago., & H. Rasgado-Flores. Dept. Physiol. Med. Sch. Univ. MD. Baltimore, MD 21201. Scarce information is available about volume regulation in muscle cells. We studied volume and membrane potential changes in response to hyposmotic stress in isolated barnacle muscle cells. Anisotonic media were obtained by changing the concentration of sucrose. Various concentrations of Ca_o were obtained by replacing Ca^{2+} mole-for-mole with Mg^{2+}. A linear relationship was found between the ratios of volumes (experimental/initial) and of osmolalities (initial/experimental) either in the absence or presence of 11 mM Ca_o (slope:0.65 ± 0.02, intercept: 0.35 ± 0.03). Cell swelling was accompanied with membrane depolarization. In the absence of Ca_o, cell swelling lasted for as long as the cells were exposed to hypotonic media. In the presence of Ca_o (4-11 mM), however, cell swelling spontaneously decreased accompanied with membrane repolarization. After this reduction in volume, re-establishment of isotonic media produced shrinking to lower values than under isotonic conditions. This indicates that Ca_o is required for regulatory volume decrease in barnacle muscle cells.

M-Pos596

EVIDENCE FOR Na+K/Mg EXCHANGE IN SQUID GIANT AXONS. H. Rasgado-Flores., & H. Gonzalez-Serratos. Depts. Physiol. & Biophys. Univ. MD. Medical Sch. Baltimore, MD. 21201. A Na/Mg exchanger has been postulated to explain an electroneutral extracellular Na^+ (Na_o)-dependent Mg^{2+} efflux in squid axons. However, numerous observations remain unexplained by such mechanism: i) the measured free $[Mg^{2+}]_i$ is much higher than the one expected from the activity of either a 2Na/1Mg or a 1Na/1Mg exchanger; ii) extracellular K^+ activates Mg^{2+} efflux. Coupling of the electrochemical gradients of Na^+, K^+ and Mg^{2+} through a 1Na + 1K/1Mg exchanger predicts the value of $[Mg^{2+}]_i$ and is consistent with the reported observations about Mg^{2+} transport in excitable cells. To assess the existence of this Na + K/Mg exchanger, we analyzed the effect of K^+ on Mg_o-dependent Na^+ efflux in dialyzed squid giant axons. The results showed that intracellular (but not extracellular) K^+ is required for Mg_o-dependent Na^+ efflux; Mg_o promotes a simultaneous K^+ and Na^+ efflux. The ratio of the Mg_o-dependent Na^+ efflux over the Mg_o-dependent K^+ efflux is 0.98. These results suggest that a 1Na + 1K/ 1Mg exchanger is indeed present in squid axons and is responsible for maintaining $[Mg^{2+}]_i$ under steady state conditions.

M-Pos597

Cr(III)NTA COMPLEX BOTH AS AN e_{aq}^- SCAVENGER AND AN INTERNAL REFERENCE IN X-RAY SPECTROSCOPY (EXAFS). S.I. Ayene and B. Chance. Dept. Biochem. and Biophys.Univ of Penn, Phila., Pa. 19104

The trend towards more dilute samples and X-ray beams of remarkably high intensity emphasizes the need for quantitative studies of sample damage and its protection during X-ray spectroscopy. Cr(III)NTA (nitrilo tri acetic acid) complex (15 mM) was found to be an efficient internal reference in X-ray spectroscopy (Khalid, S., Chance, B. and Ayene, S.I., unpubl. data). It has been demonstrated that Fe(III) and Cu(II)NTA complexes can oxidize deoxymyoglobin to metmyoglobin (Hegetschweiler et al. 1987). Hence, Cr(III)NTA complex was tested for its efficiency to scavenge the e_{aq}^- during EXAFS. Surprisingly, this complex at a much lower concentration (1.5 mM) exhibited 95% protection against radiation-induced (300 Gy) reduction of myoglobin, cytochrome c oxidase and cytochrome c. There was no post-irradiation effect of Cr(III)NTA complex on the reduced myoglobin indicating that the protection is due to scavenging of e_{aq}^-.

The integrity of the sample in the presence of Cr(III)NTA complex was also tested using edge spectrum of X-ray absorption spectra. We found that the near edge spectrum of cytochrome c is not altered at room temperature in the presence of Cr(III) complex.

Hegetschweiler, et al., (1987) BBA 912:384-397

Supported in part by NIH Grant RR 01633

M-Pos598

GENERAL/SPECIFIC BIOSYNTHETIC RESPONSES TO ELECTROMAGNETIC STIMULATION M.Blank*& R.Goodman,**Depts.of*Physiology & Cellular Biophysics and **Pathology, Columbia University, NY,NY 10032

Changes in the MW distribution of proteins synthesized by weak electromagnetic (EM) stimulation (Blank & Goodman, Bioelectrochem. Bioenerg. 19:569,1988) are also seen in heat shock and where cell membranes have been damaged. The responses appear to be a general reaction to stress, coupled with changes that reflect the properties of the stimulus. An electrochemical model (Blank, BBA 906:277, 1987), predicts that specific responses to EM arise when the charged surfaces involved in biosynthesis experience interference. The new proteins synthesized during EM or thermal stress have properties that would be expected if they arose from an early termination of biosynthesis (Blank & Goodman, Bioelectrochem. Bioenerg. 21:307,1989). These data are in accord with the electrochemical model in that interference should increase with both the frequency of the EM and the charge on the molecules, and result in smaller polypeptides than in the control cells. (We thank the ONR and EPRI for support.)

M-Pos599

A 100 MHz DUAL WAVELENGTH PHASE MODULATION SPECTROMETER. B. Chance, M.Z. Zhang, J. Sorge, J.S. Leigh, D. Kurth & S. Nioka. Dept. Biochem. and Biophys., University of Pennsylvania, Phila., Pa. 19104

Pulse-time measurements of optical path lengths of photon migration (1) (TRS) of brain and muscle give precise values of hemoglobin/myoglobin concentration changes in normoxia and hypoxia (2,3). The bulky laser apparatus is unsuitable for clinical studies. A phase modulation system activates laser diodes at 754 and 816 nm at two frequencies near 100 MHz. Fiber optic coupling to the forehead and to an R928 PMT with dynode carrier modulation allows measurement of the time delay of photon propagation at the two wavelengths. The noise level (1 Hz band width) is less than 4 ps and the drift rate less than 4 ps/min. Concentration changes are calculated by TRS from the slope of the exponential decay (μ) and by PMS from the relationship $\mu = 0.03/\tan\phi$ based upon an RC circuit model and verified for a yeast/blood system. In a piglet brain, the incremental delays in normoxia and anoxia measured by the two systems, TRS and PMS, are respectively 96 and 91 ps. Similar results are obtained with multifrequency PMS in collaboration with Drs. Lakowitz and Berndt (NSF Center for Fluorescence Spectroscopy). 1) Blumberg, W.E. (1987) BiophysJ. 51:288a; 2) Chance, B. et al. (1988) Proc.Natl. Acad.Sci.USA 85: 4971-5; 3) Chance, B. et al. (1988) Anal. Biochem.174:698-707. Support in part: NIH Grants & NS 27346 M.Zhang supported by NS 26975.

M-Pos600

A METHOD FOR ON-LINE BACKGROUND SUBTRACTION IN FREQUENCY DOMAIN FLUOROMETRY

G.D. Reinhart[1], B. Feddersen[2], D.M. Jameson[3], and E. Gratton[2]

[1]Dept. Chem. Biochem., Univ. of Oklahoma, Norman, OK 73019

[2]Physics Dept., Univ. of Illinois, Urbana, IL 61801

[3]Dept. Biochem. Biophys., Univ. of Hawaii at Manoa, Honolulu, HI 96822

Time-resolved fluorescence determinations on biochemical samples are sometimes complicated by contributions from background. In the time-correlated single photon couting method, on-line background subtraction is a routine procedure. A limitation of frequency domain fluorometry, however, has been the difficulty of performing this operation. We have devised a method for such on-line correction in the frequency domain, regardless of the complexity of the background decay. The method is based on the determination of the background waveform and subsequent subtraction from the sample waveform. This method is applicable to both lifetime and anisotropy decay measurements. We have demonstrated that lifetimes may be accurately recovered from samples containing background contributions ranging from less than 5% to greater than 90% of the total signal intensity. Supported by grants RR03155 (EC) and GM33216 (GDR) from the NIH and DMB8706440 (DMJ) from the NSF.

M-Pos601

HIGH-SENSITIVITY, SINGLE-MOLECULE FLUORESCENCE DETECTION IN THEORY AND PRACTICE. Richard A. Mathies and Konan Peck Chem. Dept., Univ. of Calif., Berkeley, CA 94720 and Lubert Stryer, Department of Cell Biology, Stanford University, Stanford, CA 94305

The number of emitted photons that can be obtained from a fluorophore increases with the incident light intensity and the duration of illumination. However, saturation of the absorption transition and photodestruction place natural limits on the ultimate signal-to-noise ratio that can be obtained. Equations have been derived to describe the fluorescence-to-background-noise ratio in the presence of saturating light intensities and photodestruction. To test this theory we have performed single molecule detection of phycoerythrin (PE) [*Proc. Natl. Acad. Sci. U.S.A.* **86**, 4087 (1989)]. The laser power was selected to give a mean time between absorptions approximately equal to the fluorescence decay time. The transit time was selected to be nearly equal to the photodestruction time of ~600 μs. Under these conditions the photon count distribution function, the photon count autocorrelation function, and the concentration dependence clearly show that we are detecting bursts of fluorescence from individual fluorophores as they pass through the laser beam. A hard-wired version of this single-molecule detection system was used to measure the concentration of PE down to 10^{-15} M. The approach presented here should be useful in the optimization of fluorescence-detected DNA sequencing gels and in HPLC and capillary electrophoresis.

M-Pos602

FLUORESCENCE POLARIZATION ANISOTROPY IN VARIANT-3 SCORPION NEUROTOXIN. **Christopher Haydock, Joseph C. Sharp, Salah S. Sedarous and Franklyn G. Prendergast. Department of Biochemistry and Molecular Biology, Mayo Foundation, Rochester, Minnesota 55905.**

The internal energy for rotational isomerization on the $\chi^1 \times \chi^2$ torsion plane of tryptophan-47 in variant-3 scorpion neurotoxin is computed by adiabatic mapping with harmonic constraints that localize perturbations. This internal energy closely follows the Helmholtz free energy along the $\chi^1 + \chi^2$ reaction path we previously computed by a combination of thermodynamic perturbation and umbrella sampling. We combine a Langevin model for fluctuations on the $\chi^1 \times \chi^2$ torsion plane and a molecular dynamic simulation of the indole side chain orientational fluctuations as a function of the $\chi^1 + \chi^2$ reaction coordinate to obtain an estimate of the fluorescence polarization anisotropy on a nanosecond time scale. These internal motions are compared with experimental measurements of the fluorescence polarization anisotropy of variant-3 scorpion neurotoxin in aqueous solutions of varying viscosity. **This work is supported in part by GM 34847.**

M-Pos603

MULTILINEAR ANALYSIS OF BIOCHEMICAL FLUORESCENCE.

Robert T. Ross, Bilal M. Ezzeddine, Sateesh Thampi, Elias A. Fayyad, and Sue E. Leurgans, Department of Biochemistry, BioMedical Engineering Program, and Dept. of Statistics, Ohio State Univ., Columbus OH 43210.

The intensity of fluorescence is separately a linear function of three or more independent variables, such as excitation wavelength, emission wavelength, and any treatment which alters excitation transfer or decay kinetics. The resulting multilinear models have structure which permits the mathematical dissection of spectra from complex mixtures. Gathering the large amount of data needed requires a highly stable instrument with computer control of several experimental variables and of data acquisition. Previous algorithms for analyzing multilinear data have been unreliable and have required large amounts of computing; newly developed algorithms are much more reliable and efficient. We are using the method to resolve the properties of different tryptophans in a protein and of different chlorophyll-protein complexes in higher plant thylakoids.

M-Pos604

COMPARISON OF MAXIMUM LIKELIHOOD AND LEAST SQUARES METHODS FOR THE ANALYSIS OF TIME-RESOLVED FLUORESCENCE DECAY CURVES

Ž. Bajzer, J. C. Sharp, T. M. Therneau and F. G. Prendergast, Mayo Foundation, Rochester, MN 55905.

The maximum likelihood (ML) method based on a Poisson distribution provides more accurate estimates of decay lifetimes and fractions than the weighted least-squares technique for the analysis of time-correlated single photon counting (TSPC) fluorescence intensity decay data. This is particularly true in cases of closely spaced fluorescence lifetimes and/or very small pre-exponential factors. This was shown by simulations which included instrument response functions (IRF) and Poisson noise. Hall and Selinger (J. Phys. Chem. 85(1981) 2941 and Z. Phys. Chem. 141(1984) 77) described the ML method applied to TSPC data, but restricted analysis to one and two component decays with a known number of components, and neglected the IRF. Our simulations include more components, and we find the likelihood ratio test to be reliable in determining the number of components.

Supported by GM 34847.

M-Pos605

Effects of Heart Optical Absorbance on NADH and INDO-1 Fluorescence

T.A.Fralix, F.W.Heineman, and R.S.Balaban
Laboratory of Cardiac Energetics, NIH, Bethesda, MD 20892

Intrinsic and extrinsic fluorescent probes provide valuable information on cellular function and metabolism. As these techniques are applied to intact organs and tissues, the effects of tissue absorbance must be carefully evaluated. We have characterized the effects of tissue absorbance on NADH and INDO-1 fluorescence in the perfused heart. Our results demonstrate that tissue absorbance dominates the spectral characteristics of these probes (at 400 to 450 nm) due to myoglobin and the cytochromes. Fluorescent emission from these probes as well as the excitation pathlength was demonstrated to be dependent on tissue oxygenation. This leads to misinterpretation of the fluorescence signal with hypoxia or ischemia if appropriate corrections for tissue absorbance are not made. These corrections involve using tissue isosbestic points as well as internal standards to correct for pathlength alterations.

M-Pos606

A NOVEL APPROACH FOR MONITORING TRANSMEMBRANE ION GRADIENTS IN VIVO. Robbe C. Lyon**, James Pekar*, Daryl J. DesPres*, Chrit T.W. Moonen*, and Alan C. McLaughlin**. NIH In Vivo NMR Research Center, **LMMB, NIAAA, Rockville, MD and *BEIB, NIH, Bethesda, MD.

The redistribution of sodium and potassium ions in rat brain *in situ* was monitored by NMR spectroscopy. Upon death, a small decrease in the sodium signal and a small increase in the potassium signal was observed. These changes are consistent with a partial intracellular "NMR visibility" for these spin 3/2 quadrupolar nuclei and the expected cellular influx of sodium and efflux of potassium ions. In contrast, large increases were observed in double-quantum filtered sodium spectra. These results are consistent with the theory of relaxation-allowed multiple-quantum (MQ) NMR, which predicts that strongly-relaxed ions which have reduced "NMR visibility", will have increased "MQ NMR visibility". These results suggest that MQ NMR may be more responsive than conventional NMR for the study of compartmentalized metal ions.

M-Pos607

COMPUTER SIMULATION OF 2D-NMR (NOESY) SPECTRA OF POLYPEPTIDES Istvan P. Sugar, Yuan Xu, Charles DeLisi Departments of Biomathematical Sciences, Physiology and Biophysics, The Mount Sinai Medical Center, New York, NY 10029

2D-NMR spectroscopy is proved to be a powerful method for protein structure determination. After the assignment of resonances, the determination of 3D protein structure proceeds largely on the basis of NOESY spectra (Nuclear Overhauser Effect spectroscopy). In this work we solved the inverse problem: determining the NOESY spectrum in the knowledge of the polypeptide structure.

On the basis of a semi-classical theory of 2D-NMR[1] a FORTRAN computer program has been developed to simulate the NOESY spectrum of any polypeptide. The input parameters of the program are the following: chemical shifts of protons, correlation time, the dihedral angles of the polypeptide, NOESY mixing time and machine frequency. The program assumes that the polypeptide geometry satisfies the ECEPP (Empirical Conformation Energy Program for Peptides) standard.

Reference: Macura, S. and Ernst, R.R., Molecular Physics 1980,41,95-117

M-Pos608

NMR ANALYSES OF VERY HIGH DENSITY MAMMALIAN CELLS. *R.J. Gillies, P.G. Scherer, N. Raghunand, L.S. Okerlund and J.-P. Galons.* Dept. Biochem., Univ. Ariz. Hlth. Sci. Ctr.; Tucson, AZ. 85724

For the past few years, we have been developing hollow fiber bioreactor systems to grow and maintain high-density mammalian cell cultures under conditions appropriate for high-field NMR analyses.

In the present experiments, perfusion conditions were iterated to optimize growth of hybridoma cells to maximum density. Evaluation by a variety of criteria (relaxation, double labeling, ^{23}Na NMR) indicates that these cultures were near tissue density. At these high densities, perfusion conditions are extremely critical, since minor perturbations significantly degrade ^{31}P NMR spectral quality. Reasonable ^{31}P spectra were generated in 30 seconds, and intra- and extracellular P_i were resolvable, allowing measurements of intracellular pH. (Supported by NIH grant R24 RR05265)

M-Pos609

AGE RELATED BODY REMODELING: EVIDENCE FOR "SENESCENT CONVERGENCE." Richard P. Spencer, Dept. Nuclear Medicine, Univ. Connecticut Health Center, Farmington, CT 06032.

Decreasing organ weight, size or function can be noted with the aging process. In many cases, measurements of the highest (H) percentiles decrease faster with age than the lowest (L) percentiles. In:

$$H = s.(Age) + I$$

the slope (s) is larger than that in the expression for L. That is, values appear to be converging with age. This "senescent convergence" can be illustrated by examples from the literature. The description pertains to serum vitamin B-12 levels, in which the slope of the 97.5 percentile decreases 3.47 times faster than that of the 2.5 percentile. Additional examples are the midupper arm triceps skinfold thickness in women and the circumference of the arm. A useful approach is to extract the slope and intercept and express each as a function of the percentile. $s = A.(Percentile) + d$, and similarly for I the intercept. From equations of H and L, the age of confluence of the lines of "senescent convergence" can be calculated. The concept appears of use in selected instances of remodeling associated with aging.

M-Pos610

MATHEMATICAL MODELING AND COMPUTER SIMULATION IN FREE RADICAL RESEARCH: A NETWORK THERMODYNAMIC APPROACH, Suzuki, Y. and Ford, G. D., Department of Physiology, Medical College of Virginia, Richmond, VA 23298.

Grover and Samson (Am. J. Physiol. 256, C666-C673, 1989) presented evidence for direct superoxide anion radical inhibition of the Ca^{2+}-pump of the vascular smooth muscle sarcoplasmic reticulum (SR), specifically SOD but not catalase protected SR from the effects of xanthine-xanthine oxidase produced radicals. This reemphasized the importance of the superoxide theory of oxygen toxicity proposed by McCord and Fridovich twenty years ago. To test this hypothesis, a computer simulation of oxygen free radical system was created using network thermodynamic modeling and SPICE2 (Simulation Program with Integrated Circuit Emphasis, Version 2). The simulation estimated concentrations of free radicals generated by xanthine oxidase, dismutation, and Fenton reactions. According to the simulation, the possible concentration of hydroxyl radicals generated by hypoxanthine and xanthine oxidase is at least two orders of magnitude less than the concentration of superoxide anion radicals generated in the same system. Concentrations alone, however, do not tell us the potency of radicals as inhibitors. Experiments are needed to determine affinities of these radicals to the enzyme of interest. The program also simulates the interactions of superoxide anion radicals with lactic dehydrogenase and nicotinamide adenine dinucleotides, and tests the validity of a possible experimental system in which lactic dehydrogenase and NADH are used to measure ATPase activity.

M-Pos611

SIMULTANEOUS DETERMINATIONS OF THE DISSOCIATION CONSTANT AND LIGAND CONCENTRATION IN A SOLUTION WHERE BOTH PARAMETERS ARE UNKNOWN.
Frederic Mandel, The Upjohn Company, Kalamazoo, Michigan.
Intro. by W. David Behnke

Equilibrium binding studies are often used to determine the dissociation constant (K_d) of an unknown ligand or drug. If the binding is to a single class of binding sites and the drug concentration is known, the determination of K_d is quite simple. Alternatively, if the K_d for a ligand is known, binding studies may be used to deduce an unknown concentration of ligand in a given solution. However, if neither the ligand concentration nor its K_d is known, the simultaneous determination of both parameters is less straightforward. In the present study, we have examined several sets of equations that could be used for a simultaneous determination and have derived the equations that, we feel, yield the most accurate results.

M-Pos612

A GENERAL METHOD FOR FINDING EXPLICIT RELATIONSHIPS BETWEEN PHOTOPHYSICAL MODELS AND FLUORESCENCE PARAMETERS
I.P. Sugar, J. Zeng and P.L.-G. Chong. Depts. of Biomath. Sci. and Physiol. & Biophys. Mt. Sinai Med. Ctr.NY, NY 10029, and Dept. of Biochem. Meharry Med. Coll. Nashville, TN 37208

General equations are derived to provide explicit relationships between physical models and the measurable fluorescence parameters. These equations are obtained by examining the solutions of the kinetic equations involved in the photophysical events. The non-linear model parameter estimation involves the minimization of a chi-square function. We could find a chi-square function suitable for the analysis of the frequency domain fluorescence data. The main advantage of this function is that the variances of the data can be determined analytically and it is not necessary to perform repeated experiments to determine the experimental variances. This method of finding explicit relationships between the physical models and the fluorescence data is demonstrated in two examples of pyrene fluorescence (supported by the ARO).

M-Pos613

A Mathematical Model for pH Regulation in Purkinje Fibers.

D. Eugene Lovelace, Timothy E. Breen and Milton L. Pressler, Krannert Institute of Cardiology, Indiana Univ. Sch. of Medicine, Indianapolis, IN

The regulatory mechanism for intracellular pH includes buffers, surface exchange, and H^+ uptake or release from organelles. The relative role is not established. We developed a variational calculus model with a surface H^+ exchange and intracellular H^+ sources/ sinks. The model was validated by tests for fit and random errors. H^+selective microelectrodes measured $[H^+]_i$ after NH_4Cl pulses and the transsarcolemmal flux of H^+ equivalents (H^+-eq) derived. The results were: 1) SITS-sensitive anion-exchanger began during alkalinization and turned off during acidification. The influx of H^+-eq from anion exchange (An-Ex) was a determinant of NH_4Cl acidosis. 2) Amiloride sensitive H^+-eq efflux occurred during acidification. This suggests An-Ex may compensate for H^+ losses while Na/H exchange predominates during gain of H^+. The processes may activate sequentially during exposure to NH_4Cl in Purkinje fibers.

M-Pos614

PACEMAKER NEURONS: PERIODIC AND APERIODIC RESPONSES TO PERIODIC PSPs.

E. Altshuler, A. Garfinkel, J. P. Segundo, M. Stiber, G. H. Wang — UCLA (Anatomy & Cell Biology, Brain Research Institute, Computer Science, Electrical Engineering)†

Contrary to intuition, periodic driving of an oscillator does not necessarily result in periodic responses: chaos, for instance, is possible and evidence for it has arisen in several areas of neurophysiology. We studied the effects of periodic PSPs on the discharge of pacemaker neurons, in either *i.* crayfish slowly adapting receptor organs SAO (with IPSPs), or *ii.* simulated leaky integrators (with voltage-dependent I or EPSPs). The latter allowed parametric examination of the effects of, say, PSP sign and power.

Results encountered so far follow. *a.* Phase-locking with the entraining PSPs. Small-integer ratios (e.g., 1:1, 1:2, 3:2) were common in both *i* and *ii*; larger-integer ones (e.g., 15:11) appeared in *ii*. *b.* Intermittent behavior in which the driven neuron would alternate unpredictably between a phase-locked mode and either erratic or a different phase-locked behavior. *c.* Instances of erratic behavior in which the pacemaker became highly variable and hard to describe. If these are regular oscillations, they must be of periods longer than observation times. On the other hand, they might be instances of chaos, the erratic-looking behavior that is exhibited even by simple deterministic systems under certain conditions. We are investigating these outputs, particularly the erratic ones, with procedures such as Poincaré maps in an attempt to determine their true nature, the influence of noise, and to enunciate an appropriate model.

† Support: Trent J. Wells Jr. Inc., UCLA School of Medical BRSG, Army, and DARPA.

M-Pos615

A GENERAL FORMULATION OF CHEMICAL REACTIONS IN COUPLED SYSTEMS. J.S. Shiner, Physiol. Inst. der Universität, 3012 Bern, Switzerland. Chemical reactions are notorious in that the formulation of their dynamics is apparently fundamentally different from that of other sorts of processes (mechanical, electrical, e.g.). These other sorts of processes share a common formalism, which can be cast in terms of Lagrangian dynamics extended to include a dissipation function. It will be shown here how the classical description of the dynamics of chemical reactions, mass action kinetics, can be reformulated so that they are given by the Lagrangian formulation common to other sorts of processes. This represents a unification of the theory of the dynamics of chemical reactions with that of other sorts of processes and will simplify the treatment of systems where chemical reactions are coupled to other sorts of processes (mechanochemical and electrochemical systems, e.g.). The key to the reformulation is the definitions of "resistances" for chemical reactions, which allow mass action kinetics to be recovered from the formulation. The formulation is valid for stationary and transient states arbitrarily far from thermodynamic equilibrium.

M-Pos617

HIGHLY PARALLEL IMPLEMENTATION OF AUTONOMOUS DIRECTION OPTIMIZER WITH COGNITION

O.E. Rossler, G. Kampis, W. Nadler, W. Musterle, B. Schapiro and P. Urban, Inst.Phys. Theor. Chem., University of Tubingen, D-7400

The "relational" brain described in 1974 (Lect. Not. Biomath. 4, 342-369) can be implemented in a highly parallel fashion. The environment is represented in an "analogous" (spatial) form, in the pseudosimultaneous cognitive map of 1981 (BioSystems 13, 203-209). n 2-D "stencil functions" serve to "lock" every nearest source of type i into place, so that automatically the right force field is created at the center. A purely temporal"disappointment/surprise" comparator records deviations from the 2-D stencil functions, readjusting them globally, during fast simulated action. Real (slow) action gets disinhibited only after the d/s output ceases. All of this can be implemented with but a few types of module. Several levels of spatiotemporal resolution ("tolerance") can be used simultaneously (cf. 1981 ACM Comp. Sci. Conf. St. Louis p. 34). We claim that this is how our own brain is organized functionally. The fish pandaka pygmaea with its 1 mm^3 brain, and its much larger close relative gobius niger, will be natural candidates when testing the present new design principle against reality (and improving it) will be at stake.

Work supported in part by Humboldt and DFG.

M-Pos616

THE THERMODYNAMICS OF LOCAL LINKAGE EFFECTS Enrico Di Cera Ist Fisica, Univ Cattolica, Largo F. Vito 1, 00168 Roma, Italy.

Linkage effects occurring upon ligand binding to biological macromolecules can be cast in terms of global or local descriptions. The global dimension involves the macromolecule as a whole and complies with the principles of thermodynamic stability [1]. The local dimension refers to linkage effects that can be monitored specifically at individual sites [2,3], such as redox equilibria of cytochrome molecules or protein-DNA interactions. In this dimension paradoxical violations of the second law can arise as a result of local fluctuations of thermodynamic variables. These local fluctuations may have important implications in biological systems at equilibrium or steady state [4].

1. Di Cera et al. (1988) PNAS 85, 5077.
2. Ackers et al. (1983) J. Mol. Biol. 170, 223.
3. Di Cera, E. (1989) J. Theor. Biol. 136, 167.
4. Di Cera, E. (1989) J. Chem. Phys., in press.

Tu-AM-Sym I-1

The Glutamate and Nicotinic Receptor Genes Heinemann, S., Boulter,J., Connolly, J.,Deneris, E., Duvoisin,R., Hartley, M., Hermans-Borgmeyer, I., Hollmann, M., O' Shea-Greenfield, A., Papke, R. and Rogers, S. Molecular Neurobiology Laboratory, The Salk Institute P.O. Box 85800 San Diego, California 92138.

We have identified a superfamily of genes that code for the glutamate and nicotinic receptors which are the major excitatory receptors in the mammalian brain. Previous work identified seven genes that code for subunits of nicotinic acetylcholine receptors expressed in the mammalian brain; Duvoisin, R. M., E. Deneris, J. Patrick and S. Heinemann, Neuron. 3 487-496, 1989.

The glutamate receptor system is thought to be involved in the first steps of learning and memory acquisition and is perhaps the most important excitatory receptor system in the mammalian brain. We have used an expression cloning approach to identify a family of glutamate receptor genes; Hollmann,M., O' Shea-Greenfield, A., Rogers, S.W. and Heinemann, S., Nature in press 1989.

Tu-AM-Sym I-2

MOLECULAR PROPERTIES OF VOLTAGE SENSITIVE NA^+ AND CA^{++} CHANNELS. William A. Catterall, Department of Pharmacology, SJ-30, University of Washington, Seattle, WA 98195.

Voltage-sensitive Na^+ and Ca^{++} channels mediate inward movements of Na^+ and Ca^{++} that are responsible for the depolarizing phase of the action potential. Na^+ channels isolated in functional form from mammalian brain consist of a complex of an α subunit (260 kDa) in association with a $\beta 1$ subunit (36 kDa) and a disulfide-bonded to a $\beta 2$ subunit (33 kDa). α subunit mRNA is sufficient to direct the synthesis of functional sodium channels in *Xenopus* oocytes, and mammalian cells. Ca^{++} channels isolated from skeletal muscle transverse tubules consist of an α_1 subunit (175 kDa), which is similar in primary structure to the α subunit of the Na^+ channel, and contains the receptor sites for calcium channel modulators. It is associated with disulfide-linked glycoprotein complex of α_2 (143 kDa) and δ (27 kDa), β (54 kDa), and γ (30 kDa). The homologous primary structures of the α subunit of the Na^+ channel and the α_1 subunit of the Ca^{++} channel contain 4 repeated homologous domains containing multiple transmembrane segments. Site-directed, antipeptide antibodies have been used to probe the transmembrane organization of these proteins and to identify separate sites on the Na^+ channel at which cAMP-dependent phosphorylation, binding of α-scorpion toxins, and the binding of specific antibodies modulate rapid Na^+ channel inactivation. Highly conserved S4 α-helical segments in each domain are both hydrophobic and positively charged and are postulated to form voltage-sensing elements according to a "Sliding Helix" model of voltage-dependent gating. Two size forms (α_1^{175} and α_1^{212}) of the α_1 subunits of skeletal muscle calcium channels have been identified which may have different functional properties, and sites of protein phosphorylation which may regulate calcium channel activation have been localized. These studies begin the development of a functional and topological map for the principal subunits of the voltage-sensitive ion channels.

Tu-AM-Sym I-3

BIOPHYSICAL AND MOLECULAR MECHANISMS OF POTASSIUM CHANNEL GATING Richard W. Aldrich; Department of Neurobiology; Stanford University, Stanford CA

We have studied the gating of single K^+ channels in wild type *Drosophila* muscle, *Xenopus* oocytes injected with *Shaker* mRNA, and mRNA from variants generated by *in vitro* mutagenesis. Our analysis has led to the conclusion that all of the molecular transitions after first opening, including the inactivation transition, are voltage independent and therefore not associated with charge movement through the membrane. A partially-coupled model reproduces all of the single-channel and macroscopic data. We have examined the inactivation mechanism further by constructing and analyzing the gating of mutant channels that delete different portions of the sequence in the amino terminal variable region. Some of these mutations dramatically decrease the inactivation rate whereas others leave inactivation intact, and in some cases increase the inactivation rate. Comparison of these mutants has allowed us to define a 22 amino acid region near the amino terminal that is essential for normal inactivation. Small deletions or point mutations within this region have more subtle effects on the inactivation rate, and suggest an involvement of both charged and hydrophobic residues in inactivation. Our data areß consistent with the ball and chain model for inactivation originally proposed by Armstrong and Bezanilla for voltage-gated Na channels.

Tu-AM-Sym I-4

THE SPECIFICITY OF RECEPTOR/EFFECTOR COUPLING. David E. Clapham, Mayo Foundation, Rochester, MN 55905.

Over 70 receptors are coupled to ion channels or enzymes via guanine nucleotide binding proteins. How the specificity of agonist/receptor interaction is maintained in the intracellular response is a major focus of research. In cardiac atrial cells, at least three types of receptors are linked via a pertussis toxin-sensitive G protein to the same ion channel. Furthermore, there is evidence for channel activation by both G protein α and $\beta\gamma$ subunits. $G_{\beta\gamma}$ subunits may release intermediate second messengers such as arachidonic acid. Other cardiac channels may be activated even more indirectly by fatty acids and phospholipids. The specificity of receptor/effector coupling will be discussed using the cardiac inward rectifying K^+ channel and the muscarinic-activated phosphatidylinositol pathway in transfected cell lines as models for the study of signal transduction.

Tu-AM-Sym II-1

THE ROLE OF ION CHANNELS IN STIMULUS SECRETION COUPLING IN PANCREATIC ß-CELLS.

Frances M Ashcroft, P Rorsman, PA Smith, Y Oosawa *University Laboratory of Physiology, Parks Road, Oxford, OK1 3PT, U.K.*

Metabolic modulation of ionic channels plays a central role in stimulus-secretion coupling in the pancreatic ß-cell. An increase in plasma glucose stimulates ß-cell metabolism and raises intracellular ATP levels. This inhibits ATP-sensitive K-channels (K_{ATP}-channels) leading to membrane depolarisation and the initiation of Ca-dependent electrical activity; the subsequent Ca-influx stimulates insulin release. We have used cell-attached membrane patches to record single channel currents from intact ß-cells, and the perforated patch whole-cell configuration to record whole-cell currents from ß-cells in which glucose metabolism is retained, to investigate the metabolic modulation of K_{ATP} channels and L-type Ca-channels. Our perforated whole-cell studies confirm that glucose depolarises the ß-cell, and intiates electrical activity by closing K_{ATP} channels. They further show that glucose concentrations above threshold (8-20mM) increase the action potential frequency, and thus insulin release, by further decreasing K_{ATP} channel activity. Addition of 20mM glucose to the bath solution also increases whole-cell Ca-currents by increasing the activity (NP) of L-type Ca-channels. This effect is also a consequence of sugar metabolism as it can be reversed by 30mM mannoheptulose (which inhibits glucokinase) and by 2.4 µg/ml oligomycin (an inhibitor of oxidative phosphorylation). Interaction of a metabolic product common to both glycolytic and oxidative phosphorylation is thus suggested.

Tu-AM-Sym II-2

A METABOLIC BASIS FOR GLUCOSE-INDUCED Ca^{2+} OSCILLATIONS AND INSULIN SECRETION.

B.E. Corkey, E.A. Longo, J.T. Deeney, J.G. McCormack, K. Tornheim & M. Prentki.

A metabolic model of glucose-induced insulin secretion is proposed involving ATP/ADP driven alterations in electrical and metabolic events. It is based on the finding that physiological variations in the ATP/ADP ratio and acyl CoA levels affect Ca^{2+} handling by permeabilized clonal ß-cells. A key feature of the model is metabolically driven Ca^{2+} oscillations. Oscillations are an aspect of glycolytic regulation that serves to maintain a high ATP/ADP ratio. Stimulatory glucose induced a rise in the ATP/ADP ratio and oxygen consumption of single islets and increased pyruvate dehydrogenase activity in groups of islets. Data obtained from Ca^{2+} imaging of single intact islets showed oscillations with a period of about 4 min. Increasing the glucose concentration from 3 to 20 mM increased baseline Ca^{2+} about twofold and the amplitude of the oscillations about 4-fold.

Tu-AM-Sym II-3

INTRACELLULAR Ca^{2+} IN MAST CELLS: GRADIENTS AND OSCILLATIONS IN INDIVIDUAL CELLS.

Clare Fewtrell, *Department of Pharmacology, Cornell University, Ithaca, NY 14853.*

When immunoglobulin E receptors on the surface of mast cells are stimulated with antigen, intracellular free ionized calcium ($[Ca^{2+}]_i$) increases due to both the release of Ca^{2+} from intracellular stores and influx across the plasma membrane. This is followed by exocytosis of granules containing mediators of inflammation. Using image-enhanced fluorescence microscopy we have found that the $[Ca^{2+}]_i$ responses of individual tumour mast cells are very different from one another and from the mean response of the population. After a highly variable delay, there is a rapid increase in $[Ca^{2+}]_i$ in all cells in response to antigen. Oscillations in $[Ca^{2+}]_i$ are seen in many, but not all of the cells and these are generally superimposed on a more sustained increase in $[Ca^{2+}]_i$. Transient oscillations in $[Ca^{2+}]_i$ occur even when Ca^{2+} influx is inhibited, but influx is required for the sustained increase in $[Ca^{2+}]_i$ and to maintain oscillations for more than 1-2 minutes. Sequential stimulation with different antigens evokes the same characteristic $[Ca^{2+}]_i$ response in each cell. $[Ca^{2+}]_i$ is uniformly distributed in resting cells but large gradients develop after antigen-stimulation. The differences in $[Ca^{2+}]_i$ are greatest at the peaks of the oscillations and remain synchronous in both frequency and phase over the entire train of oscillations. The amplitudes of the oscillations in $[Ca^{2+}]_i$ are largest in the nuclear region and the difference in peak amplitudes between the nuclear and cytoplasmic regions is frequently ~300nM.

Tu-AM-Sym II-4

SECRETORY GRANULE COMPOSITION IN PANCREATIC ISLET CELLS BY ELECTRON PROBE X-RAY MICROANALYSIS.

Margaret C. Foster[1], Richard D. Leapman[2], Min Xu Li[3], and Illani Atwater[3], [1]Dept. of Anesthesiology, SUNY at Stony Brook, Stony Brook NY 11794-8480 and [2]BEIB, DRS and [3]LCBG, NIDDK, National Institutes of Health, Bethesda, MD 20892.

To understand stimulus-secretion coupling, one needs to know compositions of secretory granules in functioning cells. Secretory granules of different types have characteristic compositions, a type of chemical anatomy, and, at the same time, a certain heterogeneity. Fast-freezing methods are used to preserve compositions of functioning cells and organelles at some point in time. Cryosections are freeze-dried in the electron microscope, the electron beam probes individual granules in each cell, X-ray spectra are collected and elemental compositions determined. In cryosections of fast frozen islets, both insulin-secreting beta cells and glucagon-secreting alpha cells can be studied. Beta granules have high concentrations of zinc and sulfur, and high and variable calcium concentrations. Non-beta granules, presumably alpha granules, have no measurable zinc, and higher concentrations of phosphorus and magnesium than beta granules. Although distinct cell types may be classified by secretory granule type, a few "rebel" beta granules are found in non-beta cells. It is not known what stimulates secretion of these "rebel", presumably insulin-containing, granules.

Tu-AM-Sym II-5

SYNEXIN: A NEW MEMBER OF THE ANNEXIN GENE FAMILY, IS A VOLTAGE DEPENDENT CALCIUM CHANNEL PROTEIN WITH MEMBRANE FUSION PROPERTIES.

Harvey B. Pollard, Eduardo Rojas and A. Lee Burns. Laboratory of Cell Biology and Genetics, NIDDKD, NIH, Bethesda, MD, 20892

Membranes of secretory vesicles fuse with each other and with plasma membranes during exocytosis in many different cell types. The likely role of calcium in the process in some cells is now widely accepted, and it is possible that at least one cytosolic mediator of calcium action is synexin. Recent studies have shown that calcium-activated synexin molecules penetrate directly into the bilayer while forming exquisitely selective voltage dependent calcium channels (Pollard and Rojas, PNAS (1988) 85: 2974-2978). We have recently cloned the human synexin gene and learned it to be a member of the annexin gene family. In addition to the conserved C-terminal repeat, which may be the channel, the unique N-terminal portion is a 167 amino acid segment with high hydrophobicity (Burns, et al PNAS (1989) 86: 3798-3802). We have proposed that the fusion mechanism may involve a hydrophobic bridge of synexin molecule(s) between fusing membrane partners.

Tu-PM-Sym I-1

BIOPHYSICAL STUDIES OF SIGNAL SEQUENCES.

L. M. Gierasch, C. J. McKnight, M. D. Bruch, S. J. Stradley, D. W. Hoyt, and J. D. Jones, Depts. of Pharmacology and Biochemistry, UT Southwestern Medical Center, 5323 Harry Hines Blvd., Dallas, TX 75235-9041.

While signal sequences from many organisms and many secreted proteins seem to function analogously, they nonetheless lack primary structural homology. This apparent paradox has led to the hypothesis that the properties required for signal sequence function are conformational preferences and overall biophysical characteristics such as amphiphilicity and patterns of residue type. In order to understand what properties are shared by functional signal sequences, we have synthesized peptides corresponding to signal sequences of bacterial outer membrane proteins, in both wildtype and mutant, export-defective versions. A strong tendency to adopt a stable, α-helical conformation in membrane-mimetic environments and a high affinity for phospholipid monolayers and bilayers are characteristics of functional signal sequences. Furthermore, the signal peptide from the LamB protein can confer a high affinity for lipid on a passenger--the first 28 residues of mature LamB. These results are all consistent with models for protein export in which one of the roles of the signal sequence is to insert into the membrane bilayer and facilitate the initiation of translocation of the mature chain.

Supported by grants from the NIH and the NSF.

Tu-PM-Sym I-2

LIPID INVOLVEMENT IN PROTEIN TRANSLOCATION

B. de Kruijff
Centre for Biomembranes and Lipid Enzymology and Institute of Molecular Biology and Medical Biotechnology, University of Utrecht, Padualaan 8, 3584 CH Utrecht, NL

Lipids form the general permeability barrier of membranes and as such compartmentalize cellular proteins. Specific lipid classes such as acidic phospholipids appear to play an important and direct role in protein translocation across membranes. Biophysical studies in model systems on apocytochrome c-lipid interactions give insight into the ways these lipids might function in the actual membrane translocation step. Electrostatic interactions with the lipid headgroups followed by insertion into the hydrophobic region of the membrane and the accompanying changes in polypeptide and lipid structure (non-bilayer lipids) are important elements in the models proposed for apocytochrome c translocation across the mitochondrial outer membrane and are extended towards prePhoE translocation across the *E. coli* inner membrane.

Tu-PM-Sym I-3

THE ROLE OF POLYPEPTIDE FOLDING IN PROTEIN EXPORT

G. Liu, T. Topping, S. Hardy and L. Randall
Biochemistry/Biophysics Program
Washington State University
Pullman, WA 99164-4660

We have proposed that the leader sequence functions during protein export to modulate the folding of the precursor and thus allow the export apparatus to interact with some structural element accessible only in unfolded or incompletely folded proteins. Consistent with the model is the finding that folding of the periplasmic maltose-binding protein *in vitro* is retarded by the leader peptide. Furthermore, although wild type maltose-binding protein synthesized *in vivo* without a leader does not engage the cellular export apparatus, a single amino acid substitution that significantly retards folding *in vitro* restores the ability of the protein to interact with the export factor SecB. Thus the requirement for the leader peptide in this step in the export pathway can be replaced by an amino acid substitution in the remainder of the protein.

Binding studies show that both unfolded precursor and unfolded mature maltose-binding protein interact with SecB provided that their folding is similarly retarded. Competition experiments suggest that SecB will bind a large number of unfolded proteins with high affinity but has little or no affinity for their folded forms.

Tu-PM-Sym I-4

PROTEIN IMPORT INTO MITOCHONDRIA.

S.T. Swanson and D. Roise, Dept. of Chemistry, D-006, Univ. of California, San Diego, La Jolla, CA. 92093.

The mechanism of protein import into yeast mitochondria is being studied using synthetic presequence peptides. The peptides, corresponding to targeting signals from matrix-directed precursors, have been fluorescently labeled using 5-iodoacetamidofluorescein. Binding of the presequences to membrane surfaces can consequently be monitored by measuring changes in the fluorescence signal. We have used this assay to follow the interaction between presequence peptides and isolated mitochondria and to compare these interactions with the binding of the peptides to model membranes. Association of labeled peptides with proteolyzed mitochondria is being analyzed to assess the role of receptor proteins on the organelle's surface. Presequence binding to mitoplasts is being examined to define possible alternative pathways for protein import. Finally, effects of the inner membrane's electrical potential on presequence binding and translocation are being followed to define kinetic parameters for the uptake of presequences. By determining the mechanism of prepeptide association with and import into mitochondria, we hope to understand the driving force for the import of precursor proteins into the organelle.

Tu-PM-Sym I-5

GTP FUNCTION DURING PROTEIN TRANSLOCATION ACROSS THE ENDOPLASMIC RETICULUM. Reid Gilmore. The signal recognition particle (SRP) mediated transport of proteins across mammalian endoplasmic reticulum requires GTP in a capacity distinct from polypeptide elongation. We examined the role of GTP in this process by a molecular characterization of translocation intermediates that accumulate after incubation of SRP-ribosome-nascent chain complexes with microsomal membranes. SRP-receptor catalyzed displacement of SRP from the signal sequence of the nascent chain was GTP-dependent both with intact membranes and with the purified SRP receptor. The SRP receptor contains amino acid sequences which are similar to guanine ribonucleotide binding site consensus sequence elements. The GTP hydrolysis cycle of the SRP receptor was further analyzed by characterizing a SRP-SRP receptor complex that accumulates in the presence of nonhydrolyzable GTP analogues. GTP hydrolysis by the SRP receptor was stimulated by the presence of equimolar concentrations of SRP. Evidence will be presented that indicates that the affinity of SRP for the SRP receptor is regulated by the presence of bound guanine ribonucleotides.

Tu-PM-Sym II-1

CAREERS IN BIOPHYSICS. Norma M. Allewell, Wesleyan University, Middletown CT 06457.

This symposium about research frontiers and career opportunities in biophysics is being presented by the Education Committee of the Society for high school students in the Baltimore area. Dr. Robert Stroud (University of California, San Francisco) will discuss molecular recognition and its biological and clinical significance with particular emphasis on membrane receptors and enzymes. Dr. Kathleeen S. Matthews (Rice University) will discuss DNA binding proteins that act as switches for regulating gene expresssion. Dr. Steven Boxer (Stanford University) will discuss the interaction of light with living organisms, emphasizing photosynthesis and vision. Dr. Norma Allewell (Wesleyan University) will discuss strategies for selecting a college, course of study and acquiring hands on experience. The results of the poster competition will be announced and awards presented to the winners.

Tu-PM-Sym II-2

COMMUNICATION AT THE MOLECULAR LEVEL; WHY DO WE CARE?
Robert M. Stroud, University of California, San Francisco.

Tu-PM-Sym II-3

GENE EXPRESSION: SWITCHES FOR TURNING PROTEINS OFF AND ON.
KATHLEEN S. MATTHEWS (Intro. by Norma M. Allewell), Department of Biochemistry and Cell Biology, Rice University, Houston, TX 77251

Transcription of DNA sequences into complementary mRNA is the first step in producing the protein product encoded by a gene. RNA polymerase is the enzyme which carries out this copying process. One mode of modulating expression of genetic information involves recognition of specific DNA sequences by regulatory proteins. Binding of these proteins to the DNA alters the ability of RNA polymerase to transcribe adjoining sequences. This type of genetic regulation is found in all living organisms from prokaryotes to eukaryotes. Recognition of target DNA sequences by regulatory proteins can be influenced by binding of cellular metabolites or by interactions with other proteins. Complex interactive networks can be generated so that the constellation of proteins produced under particular conditions is precisely matched to the environmental and metabolic needs of the organism. The lactose and tryptophan repressors and CAP protein are examples of genetic regulatory proteins from *E. coli*. These proteins recognize specific sequences of DNA and, depending on their conformation, inhibit or promote transcription of the adjacent coding sequences by influencing initiation of transcription by RNA polymerase. In eukaryotes, a number of proteins which regulate transcription have been identified; some of these are cellular oncogenes. Maximal transcription and consequent synthesis of the encoded protein for some genes require multiple regulatory factors.

Tu-PM-Sym II-4

LIGHT AND LIFE.
Steven G. Boxer, Stanford University, Stanford, California.

Tu-PM-A1

MITOCHONDRIAL ATP SYNTHASE:PROGRESS ON THE STRUCTURE OF THE F_1 SECTOR BY X-RAY DIFFRACTION

Ysern,X, Boyington,J., Pedersen,P.,and L.M.Amzel. Dept. of Biophysics and Dept. of Biological Chemistry, Johns Hopkins University,School of Medicine, Baltimore.,MD 21205

A 3.8 A resolution map of the F_1-ATPase was obtained using crystallographic methods.The asymmetric unit contains the α and β subunits, and the whole F_1 sector is build by the crystallographic 3-fold axis. Along this symmetry axis one end of the molecule shows a cavity while at the opposite end the density is more compact and closer to the axis. The map shows regions that can be interpreted as α-helices and more than fifty chain fragments have been fitted to the density. This map is being improved by extending the data to 3.5 A resolution and proceeding through cycles of succesive steps of least squares refinement (PROLSQ), map generation with proper weighting for the partial structure (SIGMAA), rebuilding, and increasing the polypeptide backbone of the molecule. A tentative assignement of the fragments to the subunits α and β is proposed.

Tu-PM-A2

HELIX-HELIX INTERACTION IN THE TRANS-MEMBRANE F_0 SECTOR OF E. COLI ATP SYNTHASE.

Robert H. Fillingame, Michael J. Miller, Dean Fraga and Mark E. Girvin. Department of Physiological Chemistry, University of Wisconsin, Madison, WI 53706.

Subunit c (the DCCD reactive "proteolipid") is proposed to fold in the membrane as a hairpin. Mutant analysis leads us to propose that residue 24 and 28 of helix-1 lie close to the DCCD-reactive Asp-61 residue of helix 2 in the center of the membrane. Substitutions in either Ala-24 or Ile-28 reduce the reactivity of Asp-61 with DCCD. The essential carboxyl group at Asp-61 has been moved from helix-2 to helix-1 in a novel double mutant (D24,G61), and the double mutant is partially functional. Third site mutations that optimize function in the D24,G61 double mutant have been isolated, and one set of optimizing mutations localizes to the fifth putative transmembrane helix of subunit a. These results suggest that the two helices of subunit c and the fifth helix of subunit a interact during proton translocation. ^{1}H NMR studies of isolated subunit c in chloroform-methanol indicate that Ala-24 and Ala-62 lie close to each other in the folded protein (Girvin and Fillingame, these abstracts), and support the structural relationship deduced from genetic analysis.

Tu-PM-A3

ION TRANSLOCATION BY THE F_o COMPLEX.

Robert Simoni. Dept. of Biological Sciences, Stanford University, Stanford, CA 94305.

Tu-PM-A4

STRUCTURE & ORGANIZATION OF THE PLANT VACUOLAR H^+-ATPASE

H. Sze, J. Ward & S. Lai, Department of Botany, University of Maryland, College Park, MD 20742

Three subunits detected in plant vacuolar H^+-ATPases are common to all the V-type H^+-ATPases. The two major polypeptides of 72 and 60 kDa are thought to be the catalytic and regulatory subunits, respectively. The third subunit is a dicyclohexylcarbodiimide-binding proteolipid of 16 kDa. To date there is uncertainty regarding the complete subunit composition of the plant V-ATPase. In addition to the 72 and 60 kDa subunits, polypeptides of 44 and 36 kDa were removed from the membrane by washing with 0.1 M KI and MgATP. These may be additional peripheral subunits of the plant ATPase as identified by their reactivity with polyclonal antibodies to the ATPase. The molecular structure of the 16 kDa subunit from oat is being studied. Sequence analysis revealed a high degree of homology with the proteolipid of the bovine chromaffin granule V-ATPase.

Tu-PM-A5

STRUCTURE AND SUBUNIT FUNCTION OF THE COATED VESICLE PROTON PUMP. M.Forgac Dept.of Physiology, Tufts University School of Medicine, Boston, MA 02111.

We have demonstrated that the coated vesicle proton pump contains nine subunits of molecular weight 17,000-100,000 which can be immunoprecipitated using monoclonal antibodies which recognize the native enzyme. We have shown that the 73 kDa subunit functions in ATP hydrolysis while the 17 kDa subunit forms part of a DCCD-inhibitable proton channel. Determination of the subunit stoichiometry and topographical analysis using membrane impermeant reagents and immunoprecipitation have allowed us to construct a structural model for this proton pump. This model has been refined by further structural analysis of the purified, reconstituted enzyme. Our results indicate a striking similarity in the 3-dimensional structures of the vacuolar and F_1F_0 classes of proton pumps and suggest they have been derived from a common evolutionary ancestor. Sequence analysis and immunocytochemical studies also support structural similarities between the proton pumps present in different intracellular membranes.

Tu-PM-A6

Insertional Inactivation of the Genes Encoding Subunits B and *c* of V-ATPase from Yeast.
H. Nelson, T. Noumi and N. Nelson.
Roche Institute of Molecular Biology, Roche Research Center, Nutley, NJ 07110.

Vacuolar H^+-ATPase (V-ATPase) is present in the vacuolar network of eukaryotic cells and it is the ATP-synthase in archaebacteria. Like the F-ATPases that are present in eubacteria, chloroplasts and mitochondria, V-ATPases are multisubunit enzymes with distinct catalytic and membrane sectors. The genes encoding the B (57 kDa) subunit of the catalytic sector and the proteolipid (16 kDa), which is subunit *c* of the membrane sector, were cloned and sequenced. Both genes were shown to exist as single copies in the yeast genome. Each of the two genes were interrupted in haploid cells and the resulting mutants were analyzed. Both mutants exhibited identical phenotype that failed to acidify their vacuoles. The mutants did not grow in media at pH higher than 6.5, and grew well only within a narrow pH range around 5.5. The phenotype was used for analyzing of several deletions and single site mutations generated in the yeast proteolipid.

Tu-PM-A7

THE YEAST PLASMA-MEMBRANE [H^+]-ATPase: DEVELOPMENT OF AN EXPRESSION SYSTEM FOR MUTATIONAL ANALYSIS. R.K. Nakamoto, R. Rao and C.W. Slayman, Department of Human Genetics, Yale University School of Medicine, New Haven, CT 06510.

With the cloning of the PMA1 gene encoding the major proton-translocating ATPase of the yeast plasma membrane, site-directed mutagenesis has become an attractive method for the study of structure-function relationships. An essential requirement is a gene expression system where the mutant ATPase can be studied in the absence of background wild-type activity, and where ATP-driven proton transport can be assayed in addition to ATP hydrolysis. We report that *de novo* synthesized ATPase in the secretory vesicles of a temperature-sensitive *sec-6* strain can provide such a system.

The ATPase is fully mature in its catalytic and transport properties, and the vesicles are tightly enough sealed to permit the measurement of pH gradient and membrane potential with fluorescent probes. The chromosomal (wild-type) PMA1 gene is placed under galactose control so that it can be turned off at will, while a plasmid-borne (mutant) gene under heat-shock control is turned on; the secretory vesicles then contain only the mutant ATPase, which can be characterized in detail. Supported by NIH grant GM15761.

Tu-PM-A8

THE MITOCHONDRIAL ATP SYNTHASE OF Trypanosoma brucei. Noreen Williams* and Peter Frank, Dept. of Biochem, USUHS, Bethesda, MD 20814

The mitochondrial ATP synthase of the parasitic protozoan, Trypanosoma brucei has been isolated and is being characterized. The F_1-ATPase we have isolated from T. brucei is a complex composed of five subunits with component molecular weights of 55 kD, 42 kD, 32 kD, 22 kD, and 17 kD. It possesses ATPase activity with a V_{max} of 22.96 μmol/min/mg protein and a K_m value of 0.60 mM (in the standard Tris-HCl coupled enzyme assay). The soluble ATPase activity is cold labile and is not susceptible to oligomycin inhibition as is the membrane bound enzyme. The F_1-ATPase when reconstituted with F_1-depleted membranes (urea particles) regains both oligomycin sensitivity (to the same extent as that found in intact inner membrane vesicles) and regains ATP synthetic activity.

Recently we have isolated and begun characterization of both the intact ATP synthase [F_oF_1-ATPase] and the membrane moiety, the F_o. Experiments are now being conducted to determine the subunit structure of the membrane component of the H^+-ATPase and functionally reconstitute F_o and the complete H^+-ATPase in liposomes.

Tu-PM-A9

MODIFICATION OF TYR-α244 IN NONCATALYTIC SITES WITH FSBεA INACTIVATES THE BOVINE HEART F_1-ATPase

J.G. Verburg & W.S. Allison
Dept. of Chem., UCSD, La Jolla, CA 92037

The bovine heart F_1-ATPase (MF_1) is inactivated by 5′-p-fluorosulfonylbenzoyl*ethenoadenosine* (FSBεA). The dependence of the initial rate of inactivation on the concentration of FSBεA revealed a K_d of 0.25 mM for the reagent. Isolation and sequencing of labeled peptides from peptic and cyanogen bromide digests of MF_1 inactivated with [^{3}H]FSBεA showed that modification of Tyr-α244 is responsible for inactivation. Maximal inactivation of MF_1 by [^{3}H]FSBεA was correlated with derivatization of Tyr-244 in 1-2 copies of the α subunit. The following suggest that Tyr-α244 is present at noncatalytic sites which are specific for adenine nucleotides. 1) Prior modification of three noncatalytic sites with FSBA, prevented labeling of the Tyr-α244 with [^{3}H]FSBεA. 2) After maximally inactivating the capacity of MF_1 to hydrolyze saturating ATP by treatment with FSBεA, the modified enzyme hydrolyzed substoichiometric ATP with characteristics resembling those of hydrolysis of substoichiometric ATP by MF_1 maximally inactivated with FSBA. 3) The ITPase and ATPase activities of MF_1 are differentially sensitive to inactivation by FSBεA, as has been observed during inactivation of the enzyme by FSBA. In contrast, the ATPase and ITPase activities are inactivated at identical rates during modification of a single catalytic site by FSBI.

Tu-PM-B1

NUCLEOTIDE BINDING SITE TRANSITIONS IN ENERGY COUPLING BY THE Ca^{2+}-ATPase OF SR

Mervyn C. Berman, Dept. of Chemical Pathology, University of Cape Town Medical School, Observatory 7925, South Africa

A number of studies indicate subintegral stoichiometries for the Ca^{2+}-ATPase of skeletal SR under various conditions of reversible and irreversible uncoupling. Possible mechanisms include alternate catalytic cycles, slippage, or Ca^{2+} leakage via the ATPase that is not linked to ATP synthesis. Stoichiometries for Ca^{2+} and Sr^{2+} transport are similar (1.6-1.8) even though Sr^{2+} gradients do not support ATP synthesis. Access of nucleotides and H_2O to the nucleotide site has been probed by intramolecular crosslinkage (Ross and McIntosh, 1988) and by TNP-ATP fluorescence. The nucleotide site of $E_1{\sim}P.Ca_2$ is readily accessible, whereas E_2-P Ca_2 or E_2-P is inaccessible to both nucleotides and H_2O. Uncoupled preparations of ATPase show enhanced hydrophobicity in the E_2-P state, whilst phosphorylation from ATP or P_i is unaffected. An uncoupled pathway for ATP hydrolysis appears to bypass the coupled E_2-P state with a hydrophobic nucleotide site. This may represent an alternate pathway that results in suboptimal coupling at low cytosolic [Ca^{2+}].

Tu-PM-B2

FLASH PHOTOLYSIS OF CAGED-CALCIUM FOR THE STUDY OF THE CALCIUM BINDING KINETICS FOR THE SARCOPLASMIC RETICULUM ATPASE.

L.J. DeLong, C.M. Phillips, A. Scarpa†, J.H. Kaplan*, J.K. Blasie, Chemistry and *Physiology Departments, University of Pennsylvania, Philadelphia, PA 19104, and †Physiology and Biophysics Department, Case Western-Reserve University.

The kinetics of Ca^{2+} binding to the high affinity sites of the sarcoplasmic reticulum (SR) Ca^{2+}-ATP*ase* were investigated by monitoring the extravesicular calcium concentration via the metallochromic dye Arsenazo III following the release of Ca^{2+} from a photolabile caged-calcium molecule, DM-nitrophen, utilizing a pulsed Nd:YAG laser for photolysis. Two distinct SR preparations were investigated; a crude SR preparation of which ~67% of the total protein content is Ca^{2+}-ATP*ase*, and a further purified form whose Ca^{2+}-ATP*ase* content is greater than 90% of the total protein. The nature of the binding kinetics is at least biphasic over the first 500*ms* for the crude SR reaction and 200*ms* for the pure SR reaction. The stoichiometry for calcium binding expressed as Ca : $E_1 \sim P$ is better than 1:1 for a pure SR preparation under these conditions.

Tu-PM-B3

MECHANISM OF THE INHIBITION OF THE SR CALCIUM ATPase BY LANTHANUM.

William P. Jencks and Taro Fujimori, Graduate Department of Biochemistry, Brandeis University, Waltham, MA 02254.

Turnover of the SR calcium ATPase is 50% inhibited by 0.2 μM La^{3+} in the presence of 25 μM Ca^{2+} (5 mM Mg^{2+}, 0.1 M KCl, pH 7.0, 25 °C). This does not arise from binding to the Ca transport site because 100 μM La^{3+} is required to inhibit ^{45}Ca uptake in single turnover experiments. It does not occur at the low affinity Ca^{2+} site because 6.7 μM La^{3+} has no effect on the disappearance of $E{\sim}^{32}P.Ca_2$. We were puzzled by these results until we found that inhibition develops slowly over ~ 3 s (~50 turnovers). Reactivation with 0.50 mM EGTA and 0.55 mM Ca^{2+} occurs with k = 0.06 s^{-1}. Partially inhibited enzyme shows biphasic disappearance of ^{32}P-enzyme after a chase of unlabeled ATP, with k = >10 s^{-1} and 0.05 s^{-1}. The results are consistent with the slow accumulation of $Ca_2E{\sim}P.La$, which is formed slowly from phosphorylation by 0.2 μM LaATP in the presence of 50 μM MgATP, and undergoes hydrolysis with k = 0.05 s^{-1}.

Tu-PM-B4

FLUORESCENT LABELING OF THE TRANSMEMBRANE SEGMENT OF THE A1 TRYPTIC FRAGMENT OF THE SARCOPLASMIC RETICULUM (SR) ATPase IS ACCOMPANIED BY SPECIFIC INHIBITION OF CALCIUM BINDING.

C.Sumbilla, H.Malak, J.Lakowicz, and G.Inesi, Biochem. Dept., Cntr. for Fluorescence Spectroscopy, U. of Maryland, Med. Sch. Balto, MD.

SR ATPase was reacted with a fluorescent carbodiimide (NCD4) under conditions producing inhibition of calcium binding and calcium dependent phosphorylation with ATP, but not of calcium independent phosphorylation with Pi. The resulting label is localized specifically in the A1 tryptic fragment of the ATPase. Strong fluorescence energy transfer occurs between the NCD4 fluorescent label and tryptophanyl residues located within and near the transmembrane ATPase region. Negligible transfer was detected between the NCD4 label and an FITC label (Lys515) at the nucleotide binding domain. It is concluded that the NCD4 labeling associated with specific inhibition of calcium binding is located within the transmembrane segment of the A1 tryptic fragment. It cannot be excluded that crosslinking perturbations may be produced in other locations, with elimination of the carbodiimide label.

Tu-PM-B5

FUNCTIONAL CONSEQUENCES OF ALTERATIONS OF AMINO ACIDS WITHIN THE Ca^{2+} BINDING DOMAIN OF THE SARCOPLASMIC RETICULUM Ca^{2+}-ATPASE.

David M. Clarke, and David H. MacLennan, Banting and Best Dept. of Medical Research, Univ. of Toronto, Toronto, Canada, M5G 1L6.

Ligands 1 to 6 (Glu309, Glu771, Asn796, Thr799, Asp800 and Glu908 respectively) which appear to form the Ca^{2+} binding sites of the Ca^{2+}-ATPase, were altered minimally by site-directed mutagenesis. In most cases both Ca^{2+} transport and Ca^{2+}-activated phosphorylation by ATP were blocked, but phosphorylation from P_i was not inhibited by Ca^{2+}. Two exceptions were noted. A Glu for Gln replacement in ligand 6 had little effect on Ca^{2+} transport function. A Glu for Asp replacement at ligand 1 resulted in loss of Ca^{2+} transport function, but not of Ca^{2+}-activated phosphorylation. Nevertheless, Ca^{2+} phosphorylation occurred with reduced Ca^{2+} affinity. The results of the studies lend support to our hypothesis that ligands 1 to 6, believed to reside within the transmembrane domain, interact with Ca^{2+} ions during the transport process. (Supported by NIH)

Tu-PM-B6

TIME-RESOLVED AND RESONANCE X-RAY DIFFRACTION STUDIES OF THE SARCOPLASMIC RETICULUM MEMBRANE PROFILE.

J. K. Blasie, D. Pascolini, L. G. Herbette*, F. Asturias, D. Pierce and A. Scarpa‡, Dept. Chem., Univ. Penn., Philadelphia, PA 19104, *Depts. Radiol., Med. and Biochem., Univ. Conn. Health Center, Farminton, CT 06032, ‡Dept. Physiol. and Biophys., Case Western Reserve Univ., Cleveland, OH 44106.

Time-resolved x-ray diffraction experiments indicate that specific large-scale changes occur in the profile structure of the sarcoplasmic reticulum ATPase upon its phosphorylation during active transport. Several physical-chemical factors which slow the kinetics of phosphoenzyme formation induce changes in the profile structure of the unphosphorylated enzyme, opposite in general to those induced by phosphorylation. Thus, large-scale structural changes in the ATPase seem to be required for its calcium transport function. Resonance x-ray diffraction experiments identify the position of the high-affinity calcium binding sites in the ATPase profile structure. The stage is now set to follow the evolution of these sites in the ATPase profile during the "occlusion" and "translocation" steps of calcium transport via time-resolved resonance x-ray diffraction.

Tu-PM-B7

FROZEN HYDRATED CRYSTALS OF CaATPase AT 6Å RESOLUTION

David L. Stokes and N. Michael Green
Lab. of Molecular Biol., Cambridge and National Inst. for Med. Res., London, UK.

Structural studies of CaATPase have so far been restricted to low resolution due to the poor order of two-dimensional (2-D) crystal forms. However, we have found that 3-D microcrystals of detergent-solubilized CaATPase diffract to almost 4Å resolution in the electron microscope. These thin, platelike crystals have been rapidly frozen and thereby embedded in a layer of vitreous ice. By combining data from electron diffraction patterns with data from images, a 2-D density map was produced at 6Å resolution; the resolution is currently limited by the quality of images since electron diffraction extends to 4.1Å resolution. By comparing this map of frozen-hydrated (unstained) crystals with a similar map from stained crystals, we have identified separate contributions from intramembranous and extramembranous protein domains. Based on these density assignments and on the packing of molecules in the crystal, we propose an arrangement for the ten alpha-helices that have been hypothesized to span the bilayer. (supported by NIH postdoctoral fellowship)

Tu-PM-B8

THE MOLECULAR MECHANISM OF Ca^{2+}-BINDING TO SR ATPase: A FLICKERING GATE MODEL.

S. Orlowski and Ph. Champeil, SBPh and URA CNRS 1290, CEN Saclay, 91191 (France)

When $^{45}Ca^{2+}$ bound to the sarcoplasmic reticulum ATPase high affinity sites is exchanged for $^{40}Ca^{2+}$, the biphasic kinetics of this exchange allows to distinguish two sites, probably in a file in the same pocket, from which Ca^{2+} is either rapidly or slowly released. The rate of Ca^{2+} exchange at the fast site was found more sensitive to temperature, DMSO and nonylphenol than what would be expected from a Ca^{2+} pocket permanently exposed to the cytoplasmic medium. When Ca^{2+} was stripped off the ATPase by addition of EGTA, Ca^{2+} removal was strictly monophasic, suggesting that a single ion redistributes within the Ca^{2+} pocket rapidly, compared to the off rate. On the other hand, preliminary loading of the vesicles with Ca^{2+} did not affect the rate of Ca^{2+} binding to the ATPase, excluding that the Ca^{2+} sites might be accessible from the SR lumen in the ATPase unphosphorylated state. These results are discussed in relation to the suggested intramembraneous location of the Ca^{2+} sites, with special reference to a flickering gate model previously proposed for the related Na^+-K^+-ATPase.

Tu-PM-B9

MAGNESIUM IS NOT THE SOLE DIVALENT CATION FOR REVERSAL OF SR ATPase CYCLE AND ATP SYNTHESIS.

E. Mintz, J.J. Lacapère & F. Guillain,
SBPh & URA CNRS 1290, CEN Saclay, F-91191.

Calcium transport by the sarcoplasmic reticulum ATPase proceeds at the expense of Mg.ATP hydrolysis. The reversal of the cycle starts from enzyme phosphorylation by P_i and leads to ATP synthesis. We show here that the physiological co-substrate Mg^{2+} is not required for enzyme phosphorylation. Phosphoenzymes of various stability are also obtained when Co^{2+}, Mn^{2+}, Cd^{2+}, Ni^{2+} or Ca^{2+} are substituted for Mg^{2+}.

The E_2-P.Ca phosphoenzyme is unstable, because of competition between (1) the phosphorylation reaction induced by Ca^{2+} and (2) the transition induced by Ca^{2+} binding to the transport sites, which leads to an unphosphorylable conformation. DMSO and low temperature stabilize the phosphoenzyme, which may later on and under the appropriate conditions react with ADP and synthetize ATP.

The complete reversal of the cycle is thus possible without Mg^{2+}, suggesting that the phosphorylation site is not specific for the metal complexed with P_i, or ATP.

Tu-PM-B10

EVIDENCE FOR ADP-SENSITIVE (E_1P)AND ADP-INSENSITIVE (E_2P) PHOSPHOENZYME INTERMEDIATES IN THE REACTION MECHANISM OF THE CaATPASE IN SARCOPLASMIC RETICULUM (SR).

Jeffrey Froehlich and Phillip Heller.
National Institute on Aging, N.I.H.,
Baltimore, MD 21224

The generally accepted notion that the reaction mechanism of the CaATPase in SR includes two, chemically-distinct acid-stable phosphoenzyme (EP) intermediates has recently been challenged by Jencks and coworkers. We have re-examined this issue by studying the effects of K^+ and intravesicular Ca^{2+} on the kinetics of ADP-induced dephosphorylation. We find that: (1) dephosphorylation by ADP is biphasic, (2) inorganic phosphate (P_i) release is kinetically and stoichiometrically related to the slow phase of EP decay, (3) lowering K^+ increases the slowly decaying EP and associated P_i release while raising K^+ has the opposite effect, and (4) intravesicular Ca^{2+} (5mM) accelerates EP decay and P_i release, but reduces the amount of P_i liberated. These results support a model in which the initial rapid phase of ADP-induced dephosphorylation corresponds to the resynthesis of ATP from E_1P, and the slow phase represents the hydrolysis of a second acid-stable species, E_2P, that is ADP-insensitive.